The link between relative stability constant of DNA- and BSA-chromenopyrimidine complexes and cytotoxicity towards human breast cancer cells (MCF-7)

Sizwe J. Zamisa[†], Adesola A. Adeleke[‡], Nikita Devnarain[ꝼ], Mahasin Abdel Rhman[ꝼ], Peter M. O. Owira[ꝼ] and Bernard Omondi[†]

[†]*School of Chemistry and Physics, University of KwaZulu-Natal, Private Bag X54001, Durban, 4000, South Africa*

[‡]*School of Chemistry and Physics, University of KwaZulu-Natal, Private Bag X01, Pietermaritzburg, South Africa*

[ꝼ]*Molecular and Clinical Pharmacology Research Laboratory, Department of Pharmacology, Discipline of Pharmaceutical Science, University of KwaZulu-Natal, Private Bag X54001, Durban, 4000, South Africa*

SUPPLIMENTARY INFORMATION

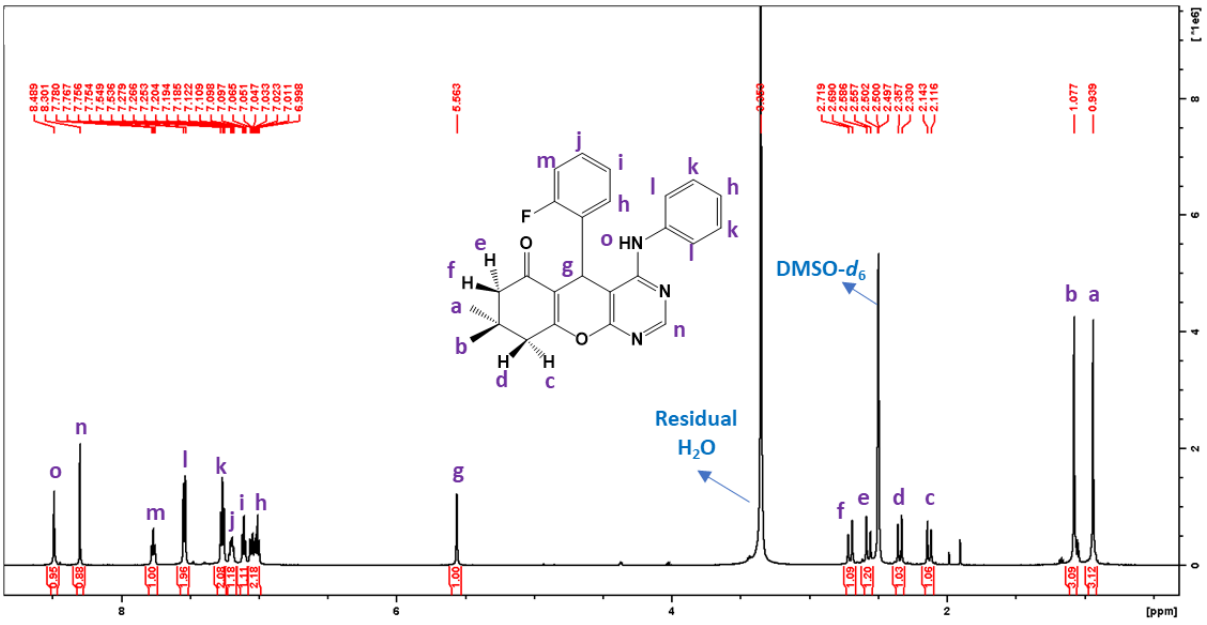

(a)

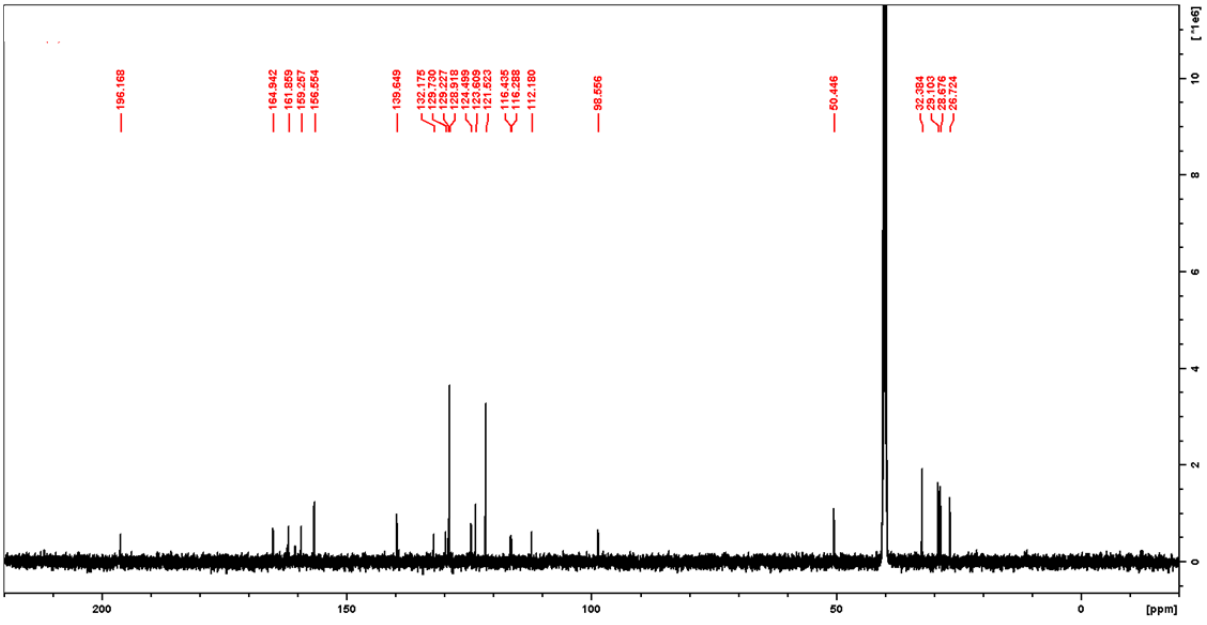

(b)

Figure S1: (a) ^{1}H NMR and (b) ^{13}C NMR spectra of **3a**

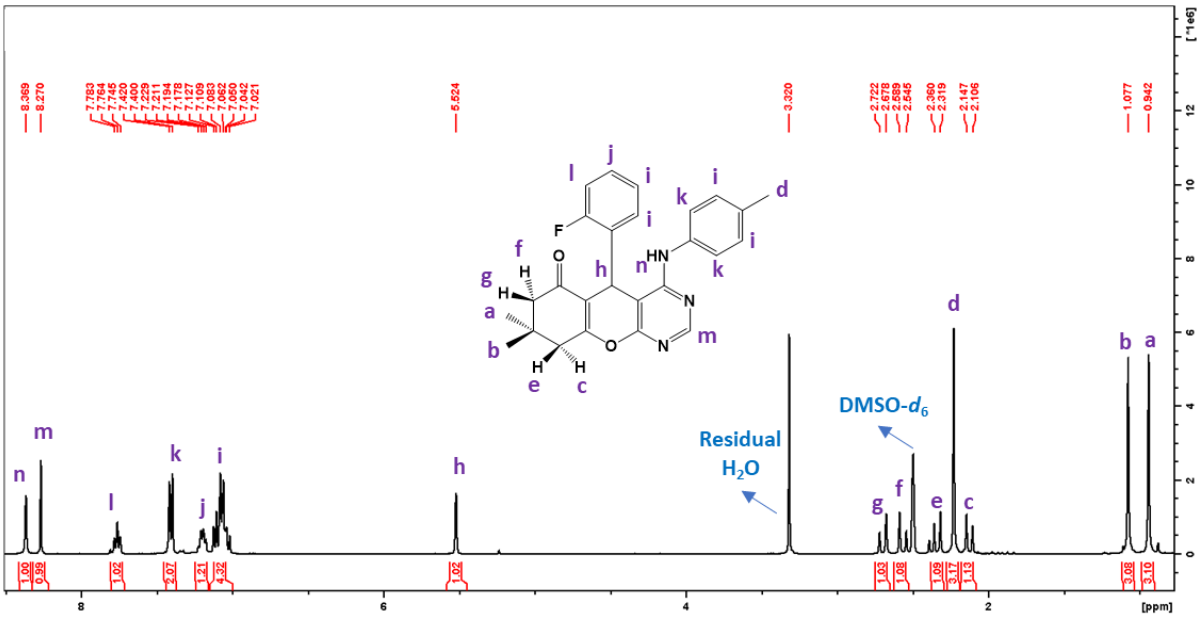

(a)

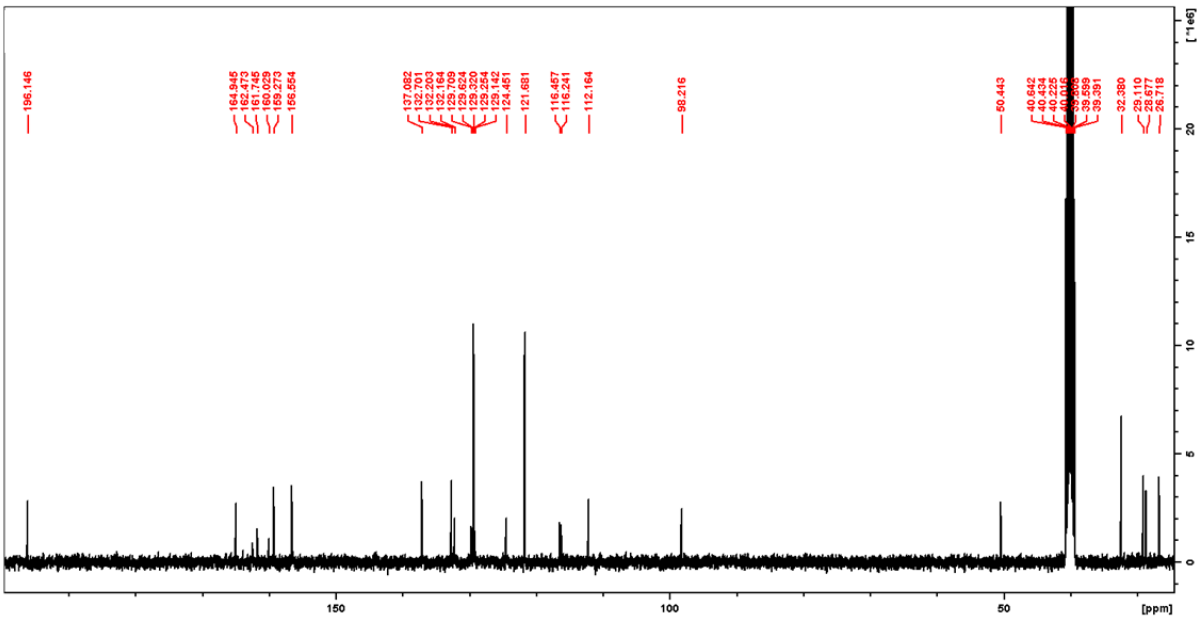

(b)

Figure S2: (a) ^{1}H NMR and (b) ^{13}C NMR spectra of **3b**

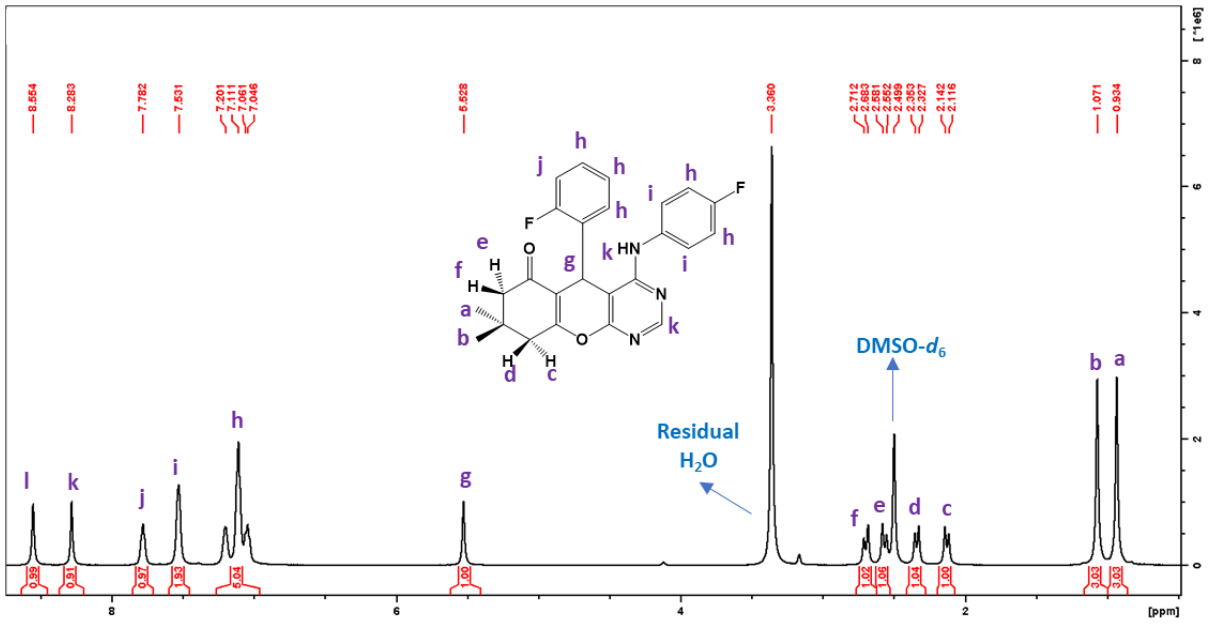

(a)

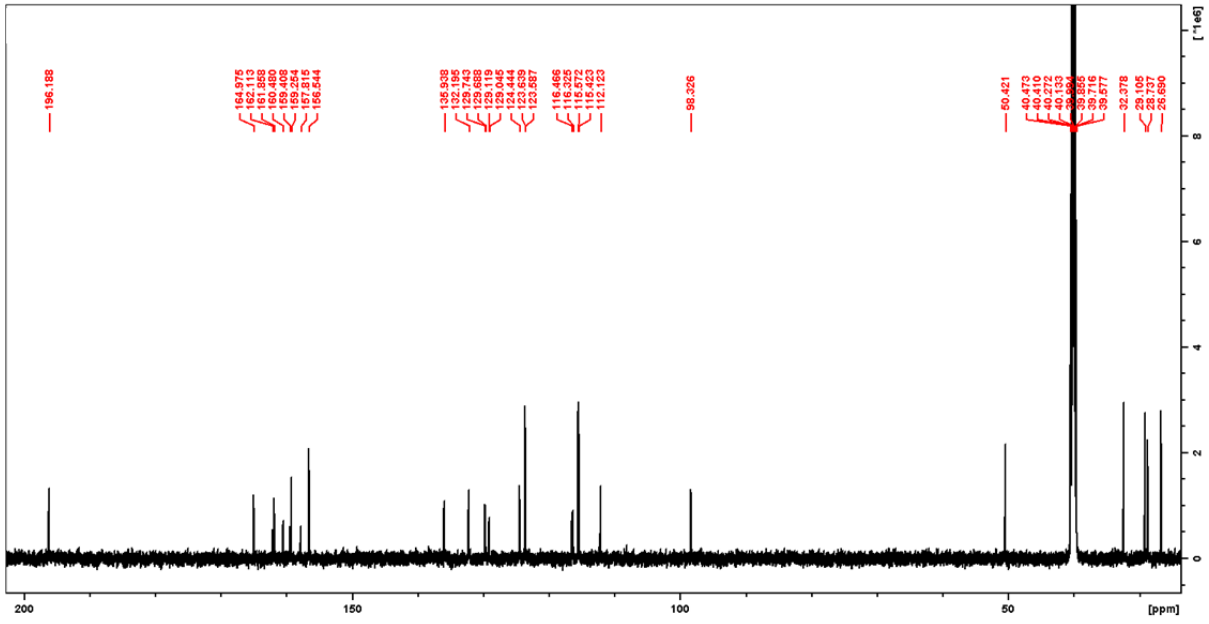

(b)

Figure S3: (a) ^{1}H NMR and (b) ^{13}C NMR spectra of **3c**

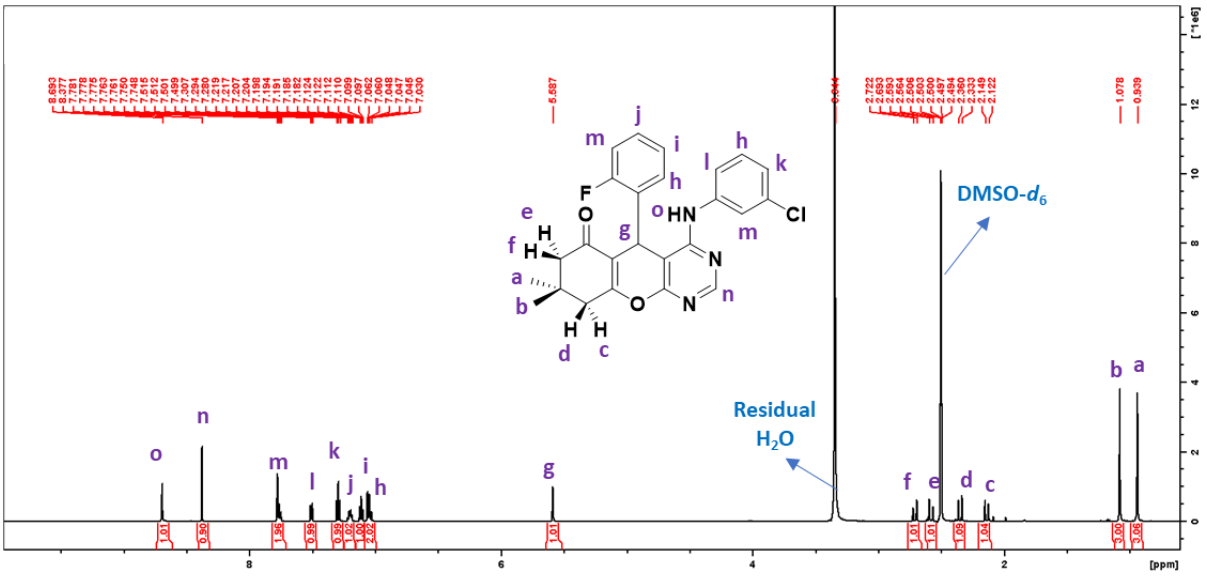

(a)

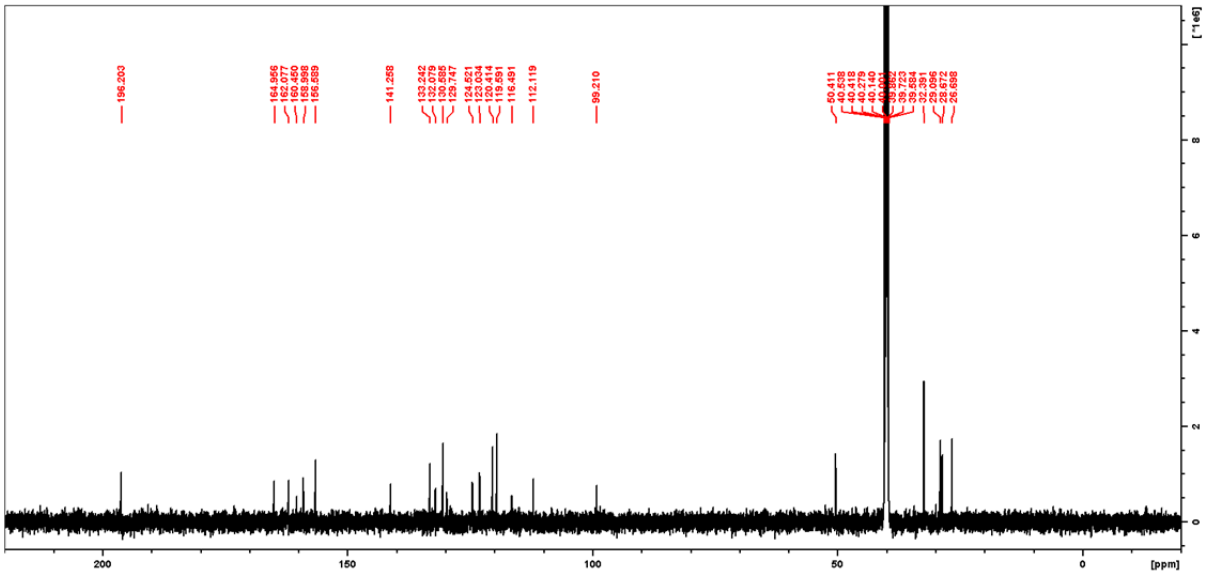

(b)

Figure S4: (a) ^{1}H NMR and (b) ^{13}C NMR spectra of **3d**

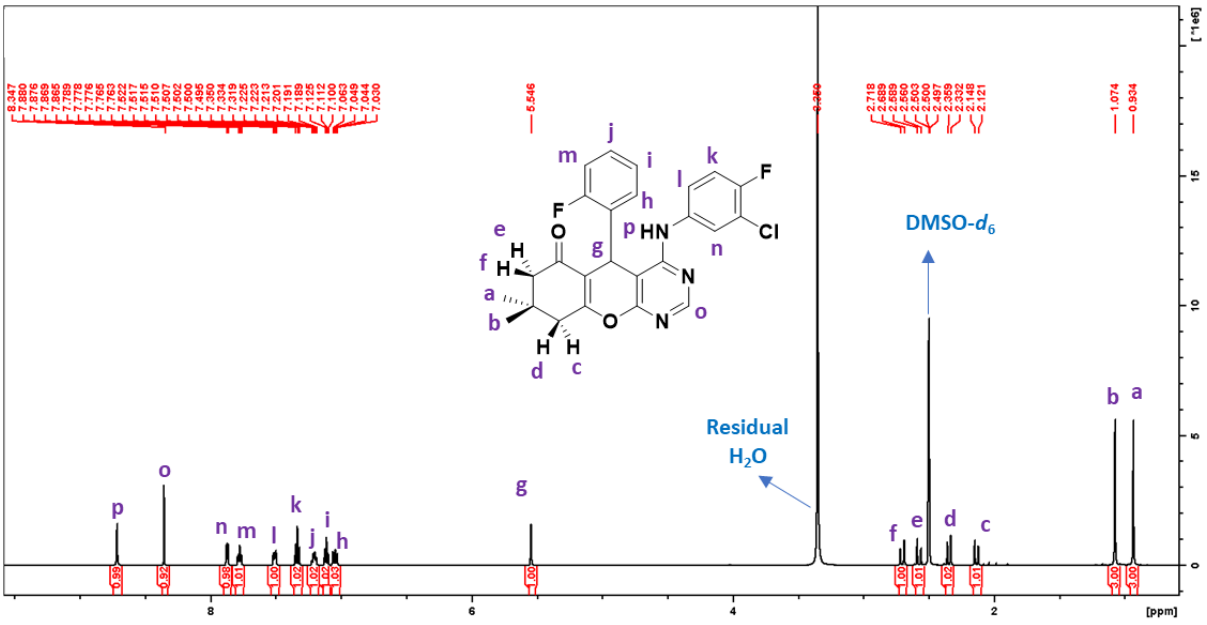

(a)

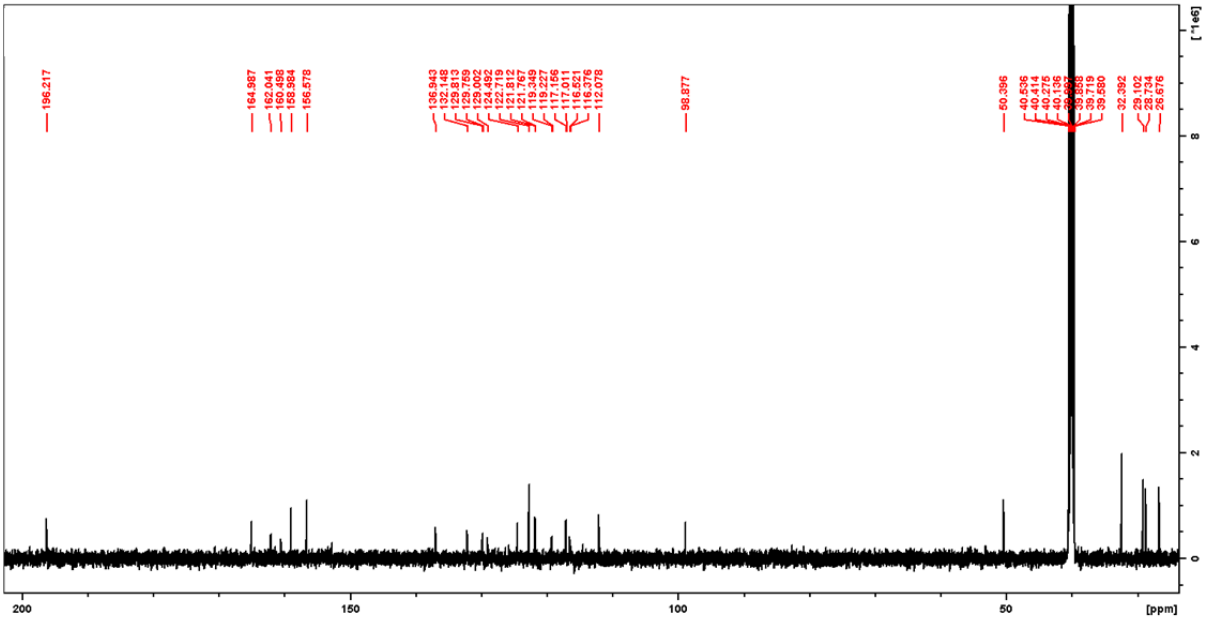

(b)

Figure S5: (a) ^{1}H NMR and (b) ^{13}C NMR spectra of **3e**

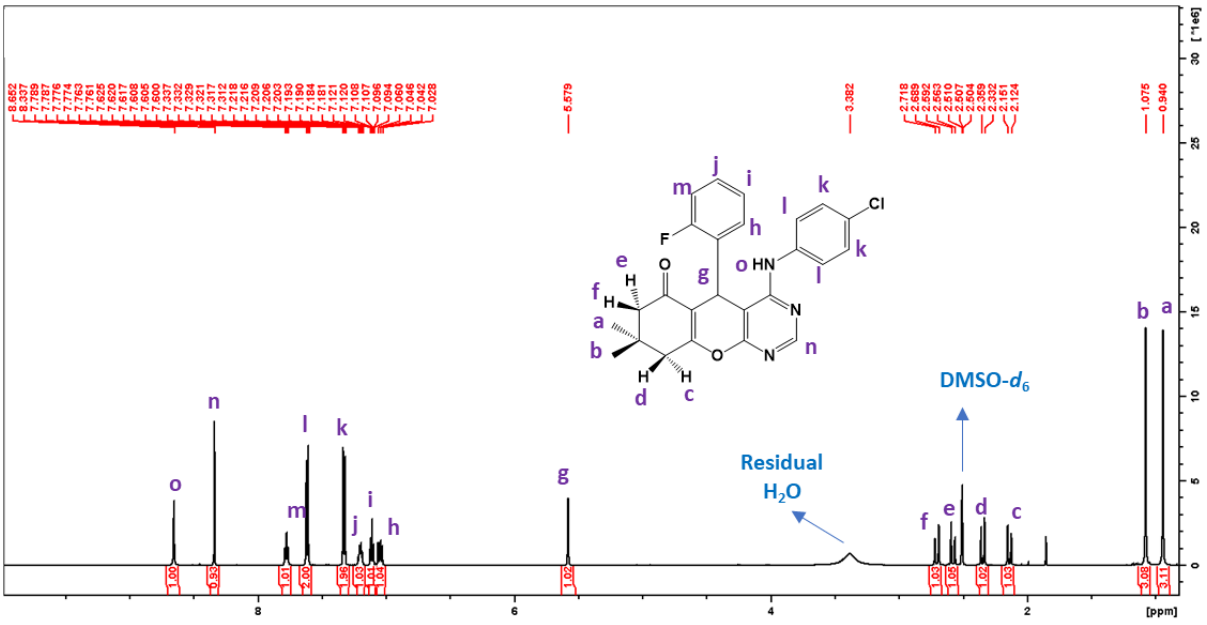

(a)

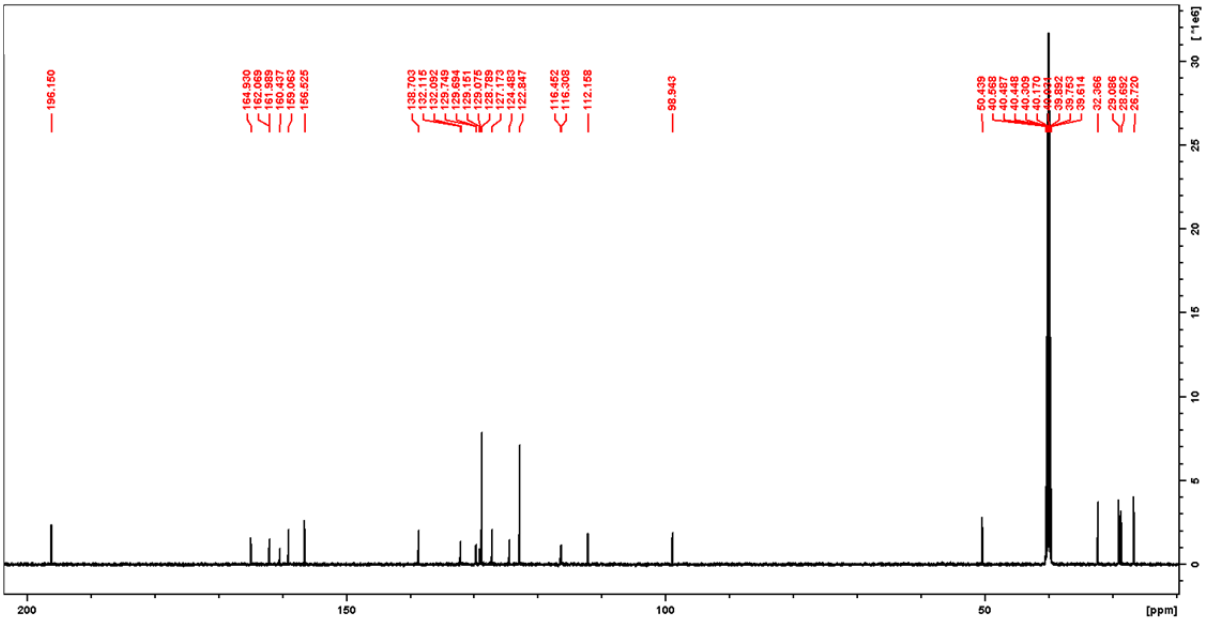

(b)

Figure S6: (a) ^{1}H NMR and (b) ^{13}C NMR spectra of **3f**

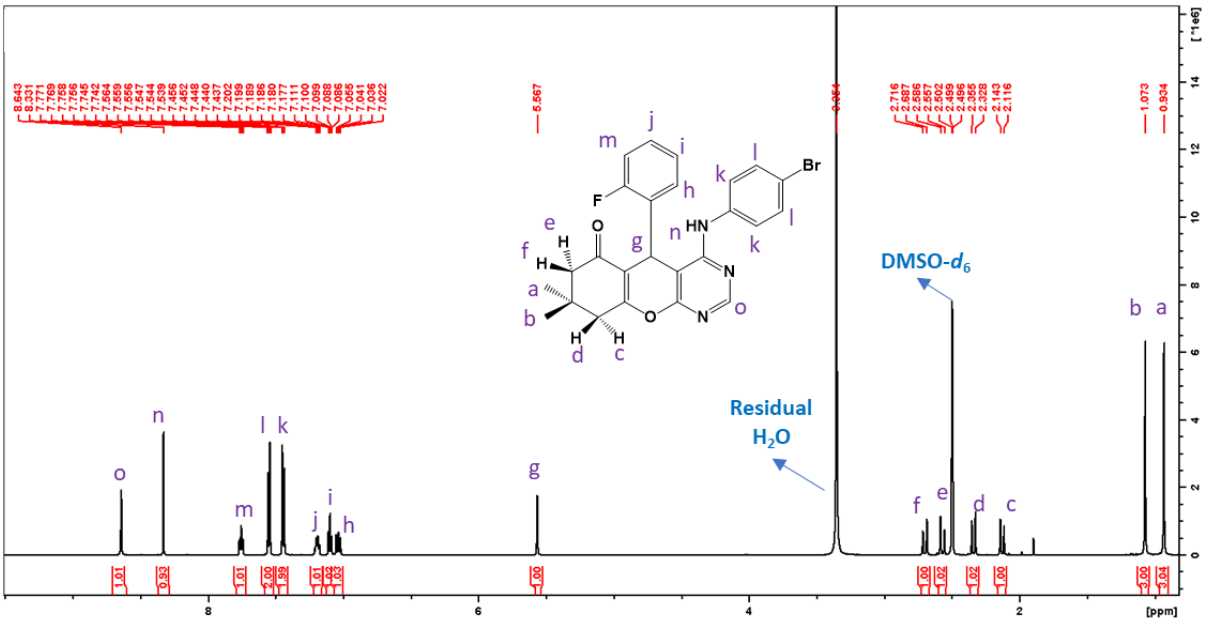

(a)

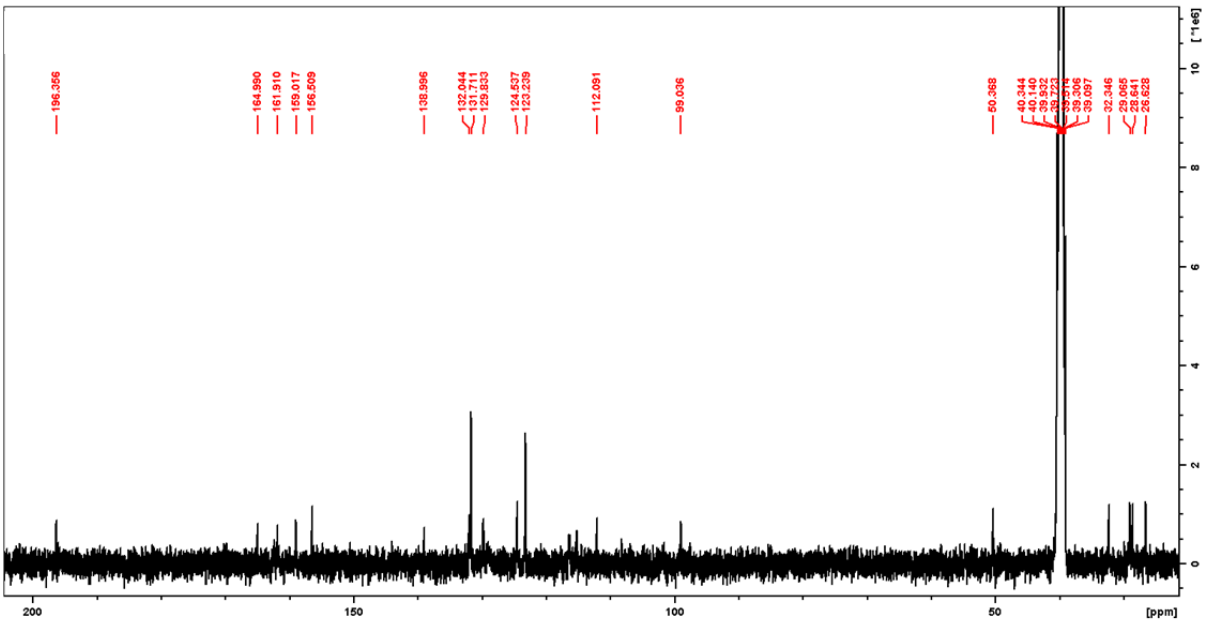

(b)

Figure S7: (a) ^{1}H NMR and (b) ^{13}C NMR spectra of **3g**

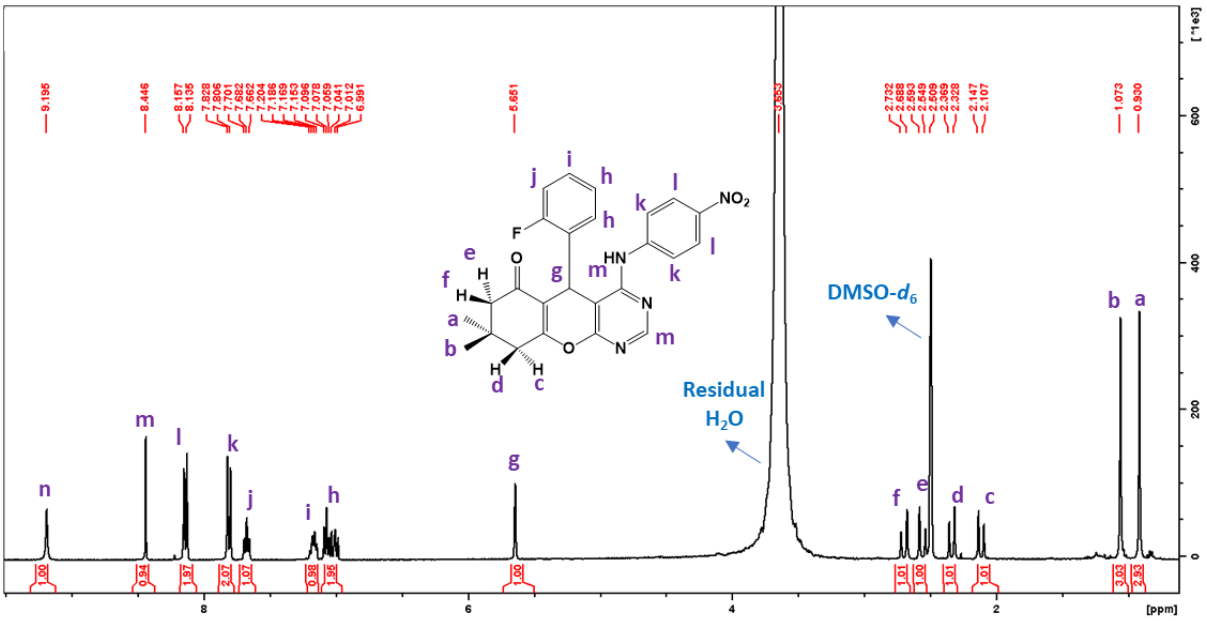

(a)

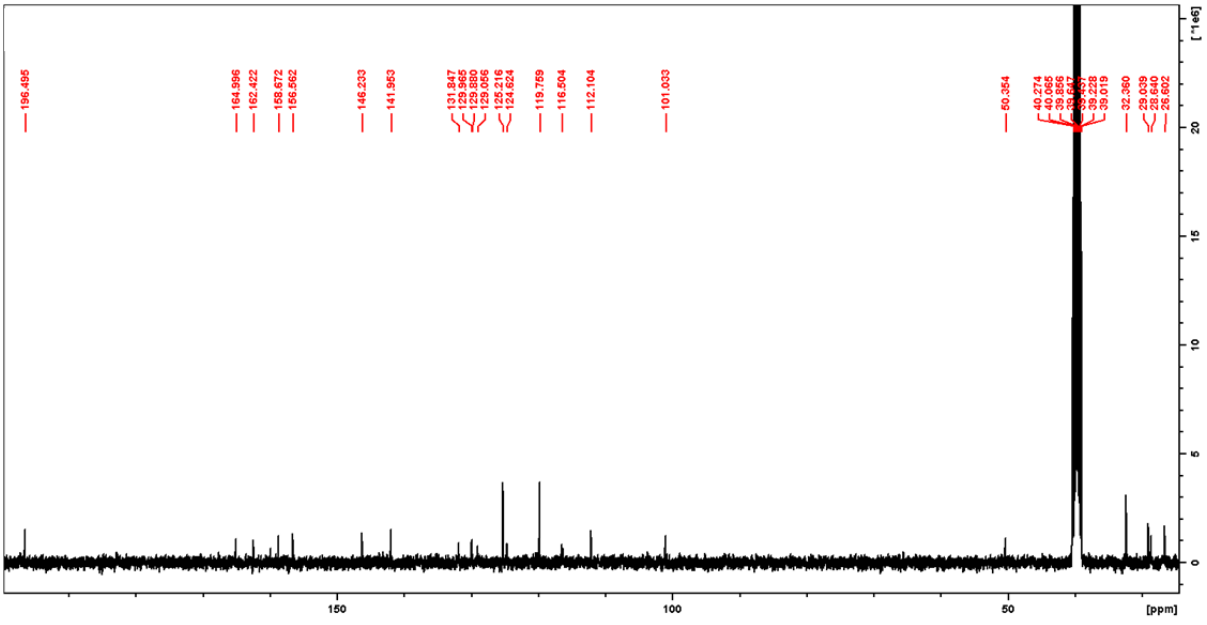

(b)

Figure S8: (a) ^{1}H NMR and (b) ^{13}C NMR spectra of **3h**

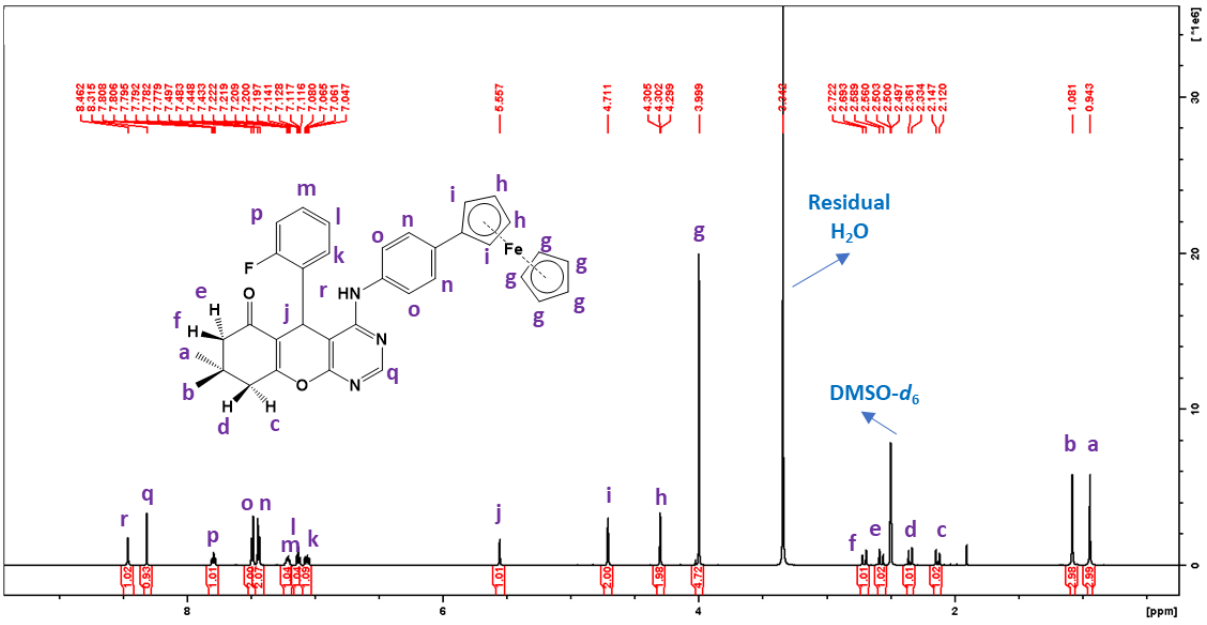

(a)

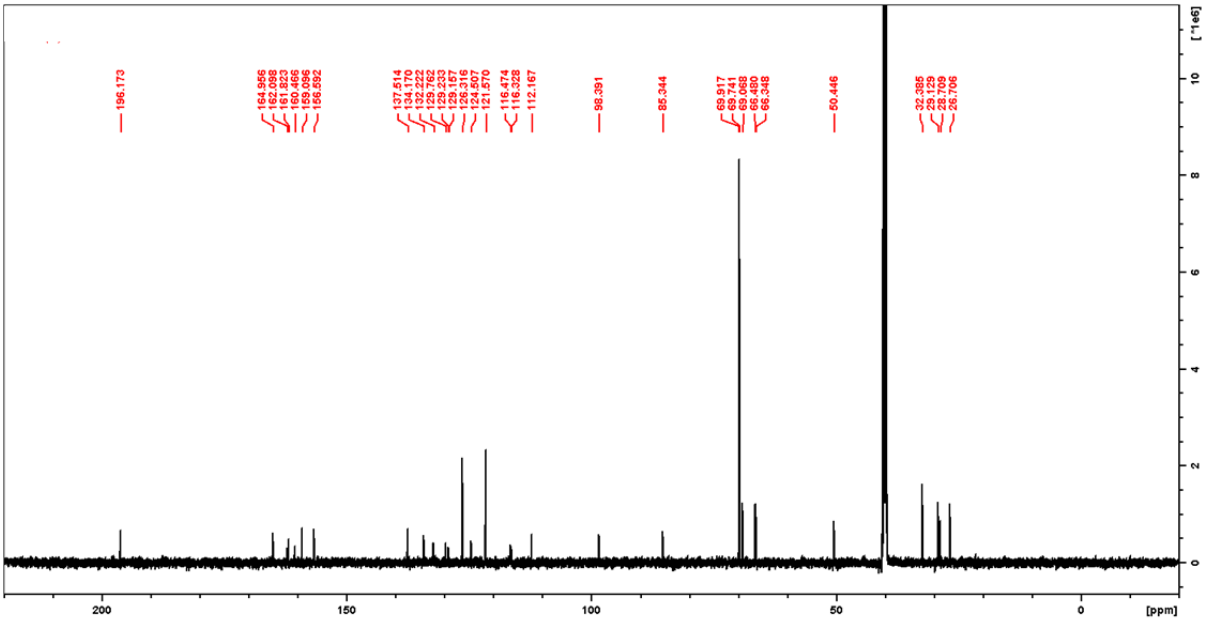

(b)

Figure S9: (a) ^{1}H NMR and (b) ^{13}C NMR spectra of **3i**

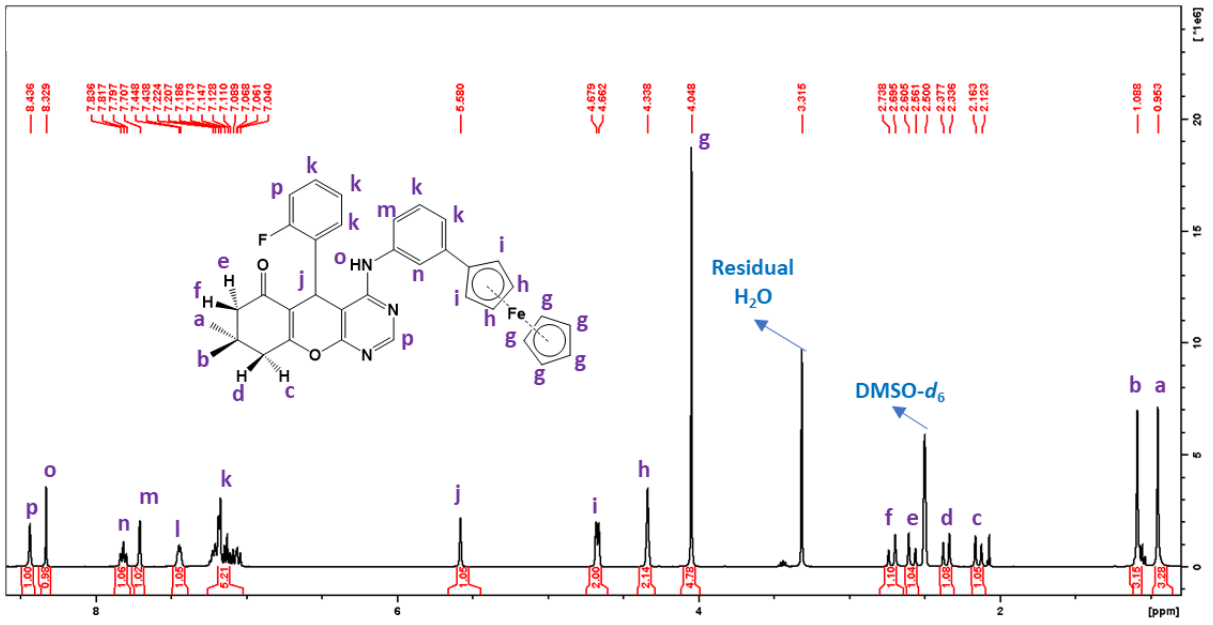

(a)

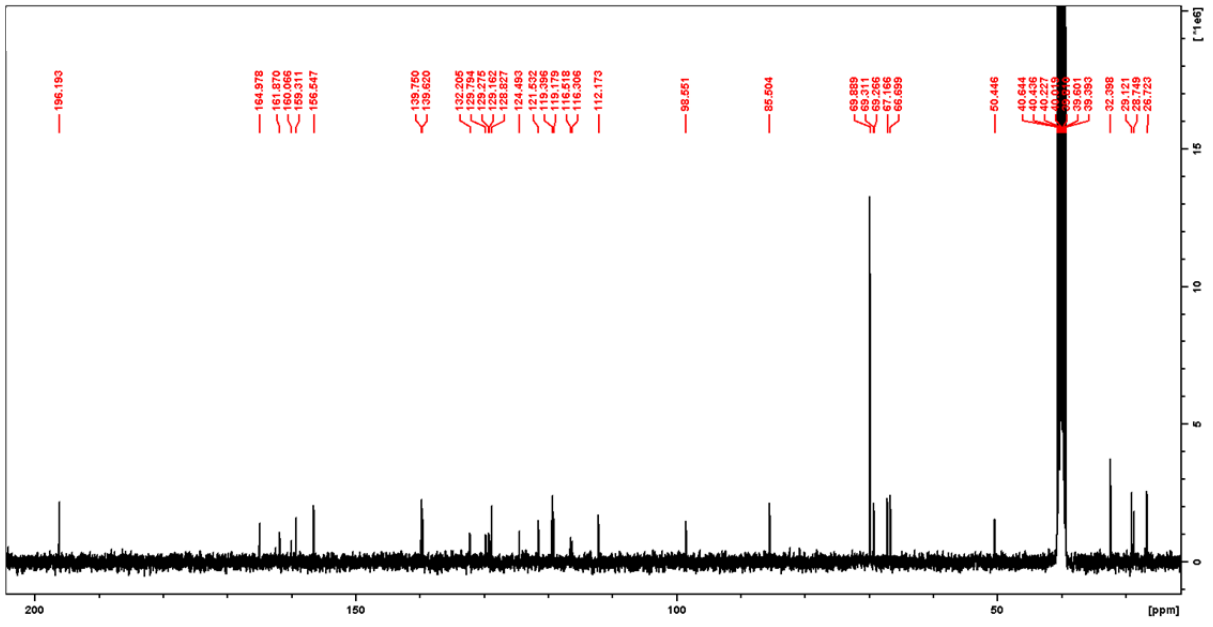

(b)

Figure S10: (a) ^{1}H NMR and (b) ^{13}C NMR spectra of **3j**

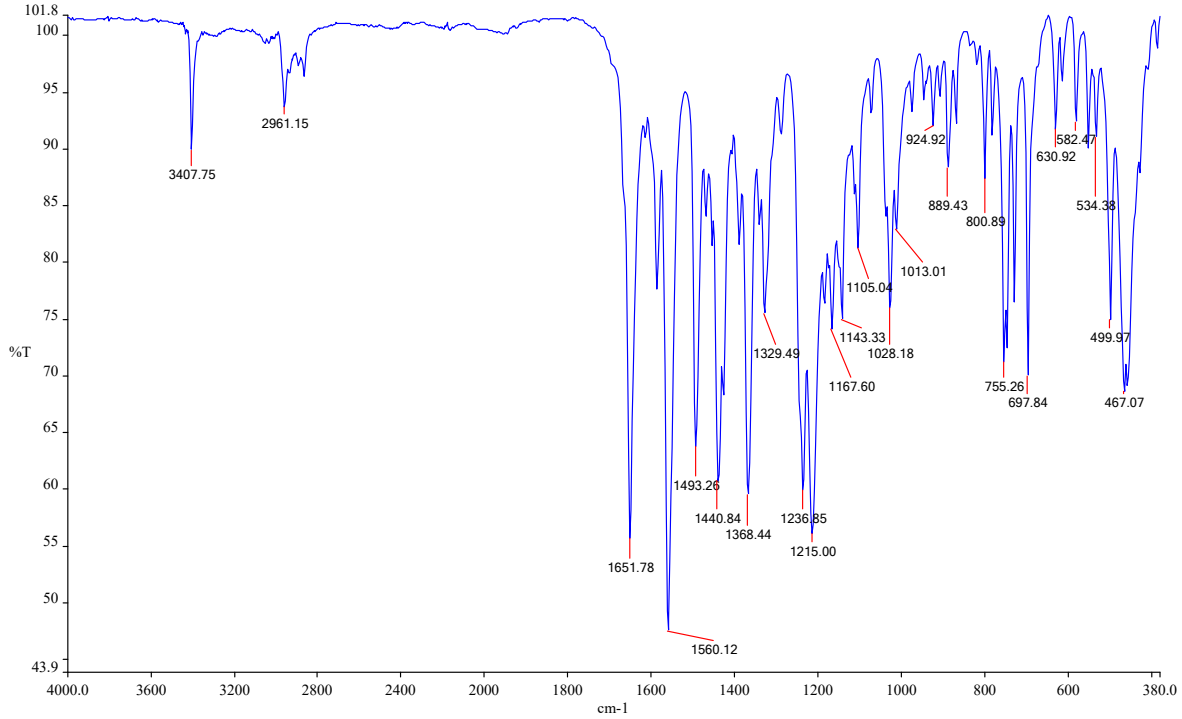

Figure S11: IR spectrum of **3a**

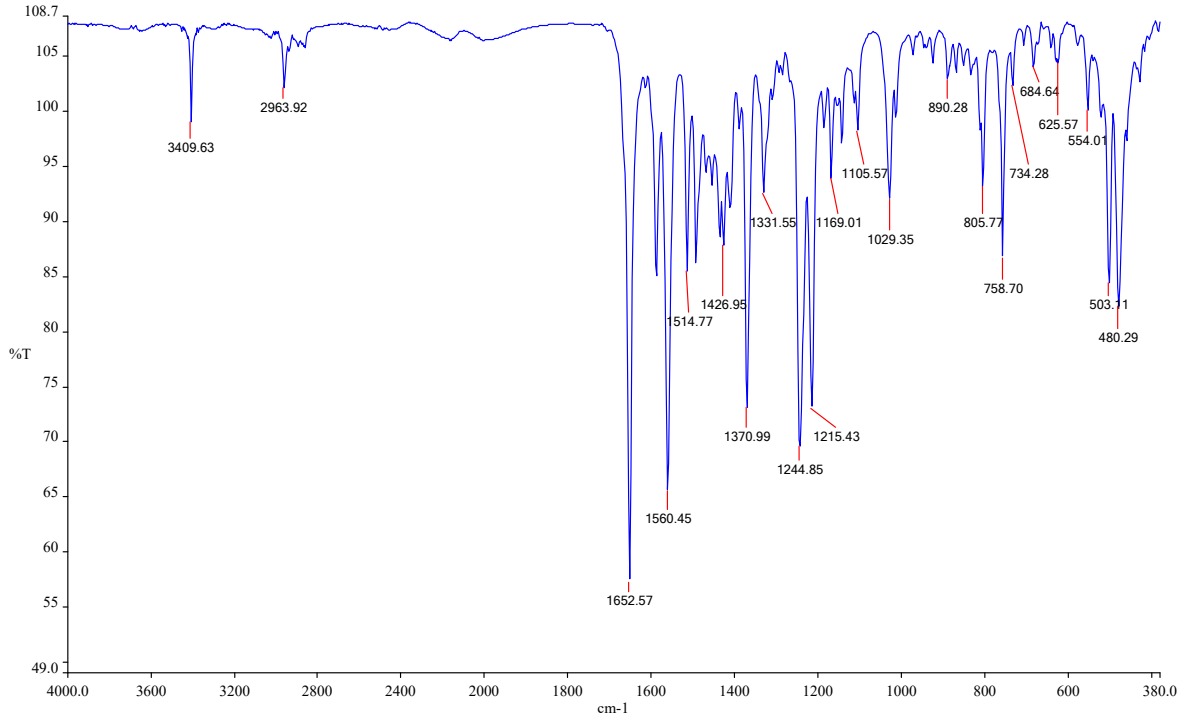

Figure S12: IR spectrum of **3b**

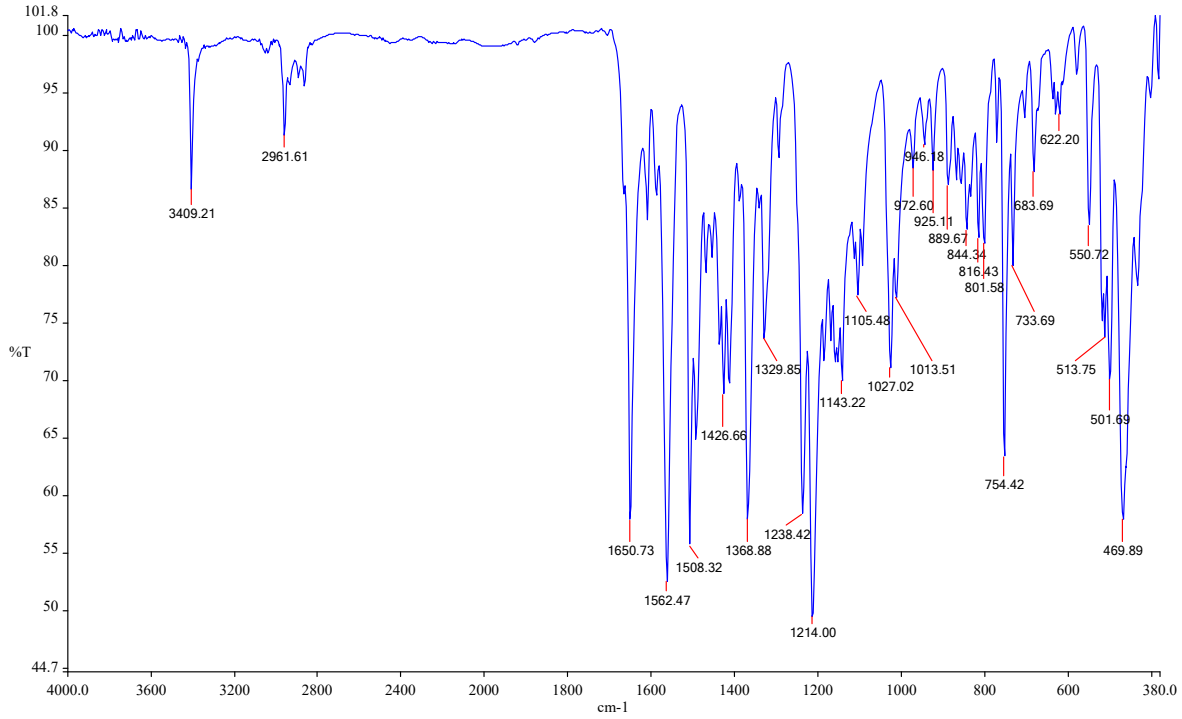

Figure S13: IR spectrum of **3c**

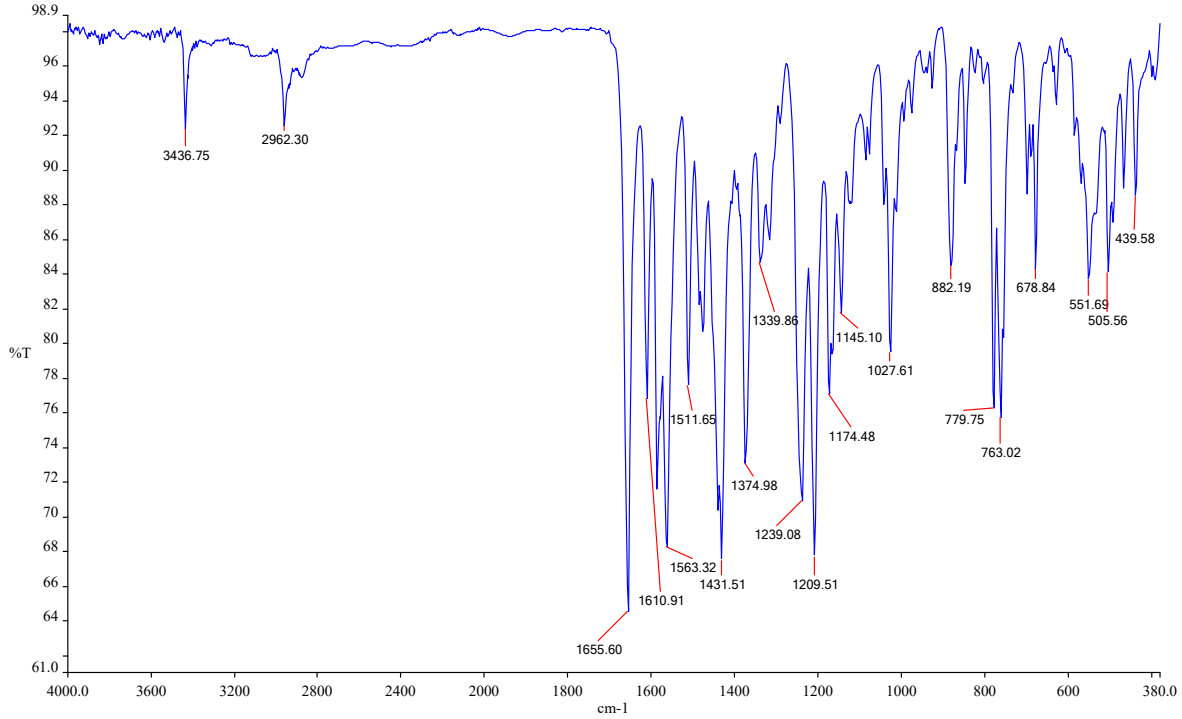

Figure S14: IR spectrum of **3d**

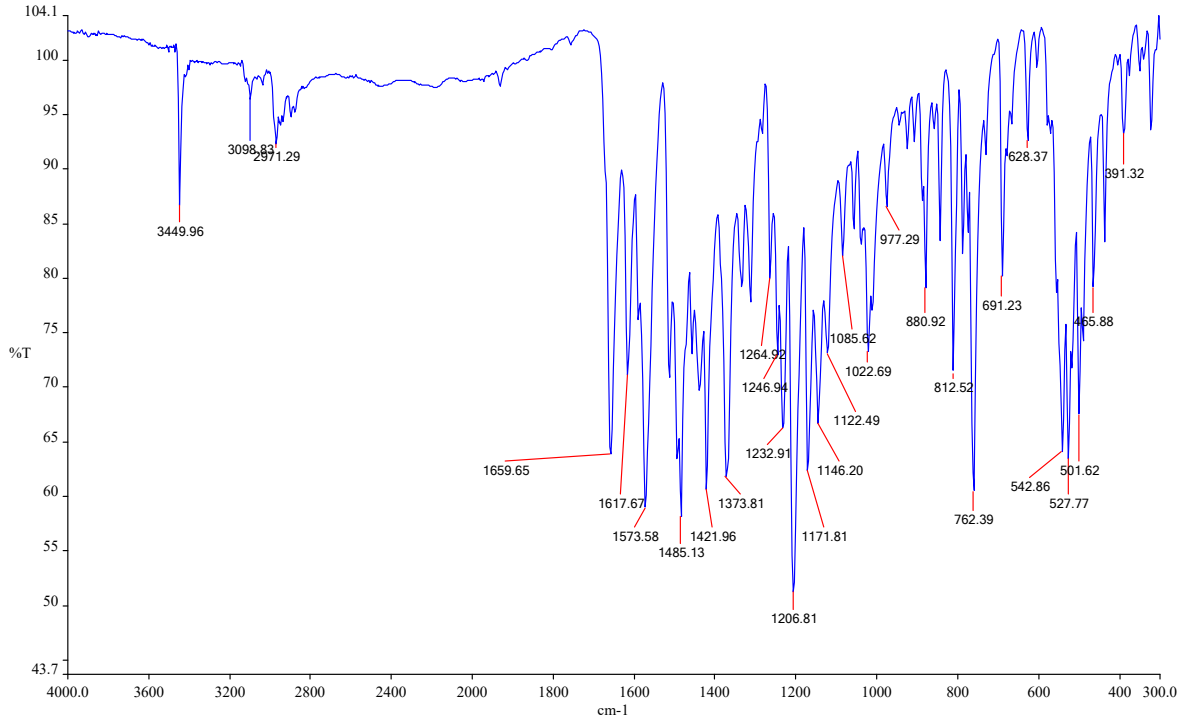

Figure S15: IR spectrum of **3e**

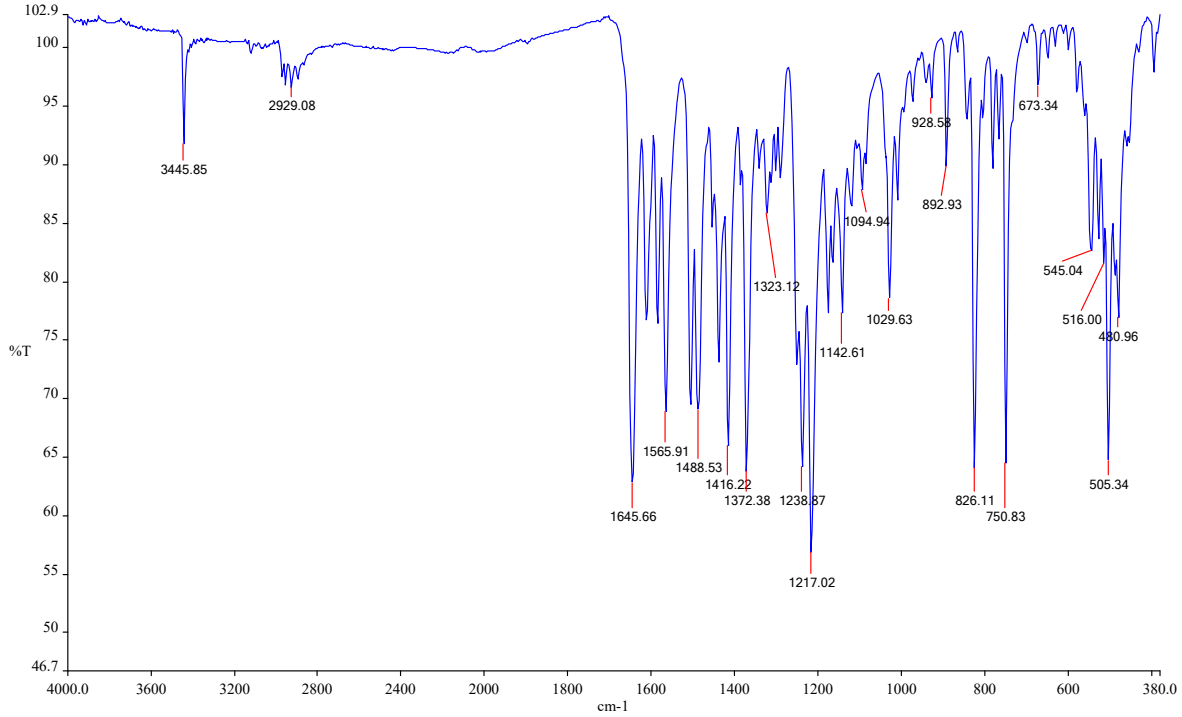

Figure S16: IR spectrum of **3f**

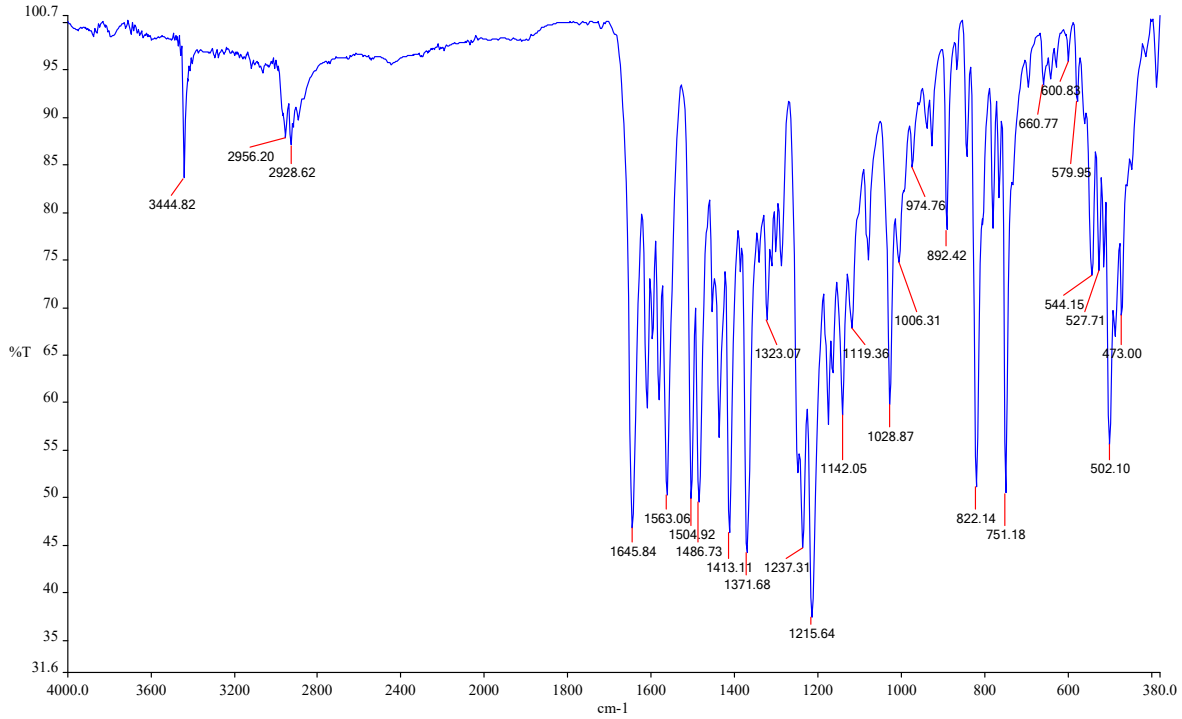

Figure S17: IR spectrum of **3g**

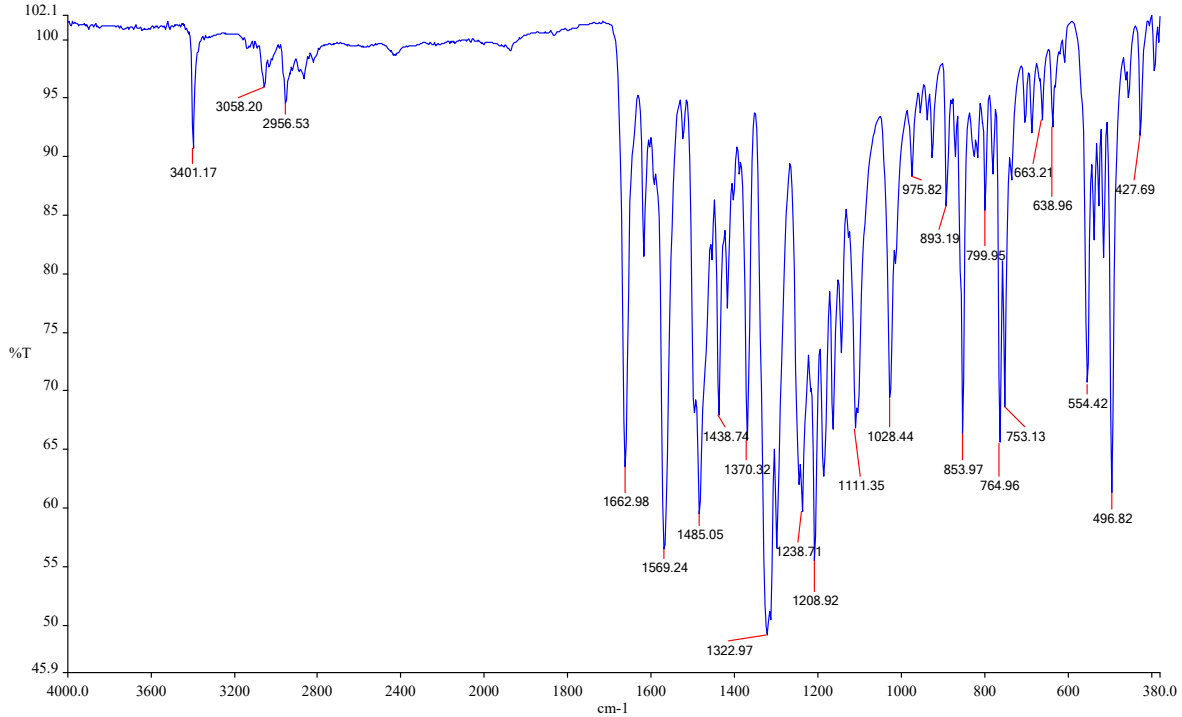

Figure S18: IR spectrum of **3h**

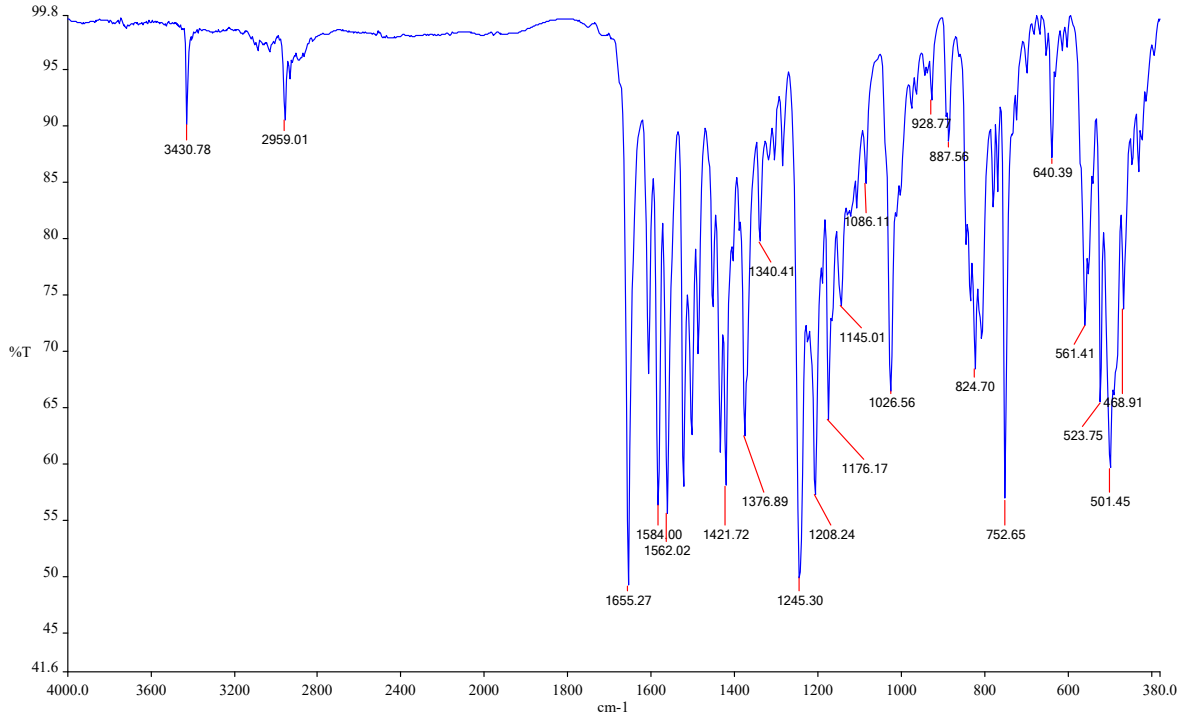

Figure S19: IR spectrum of **3i**

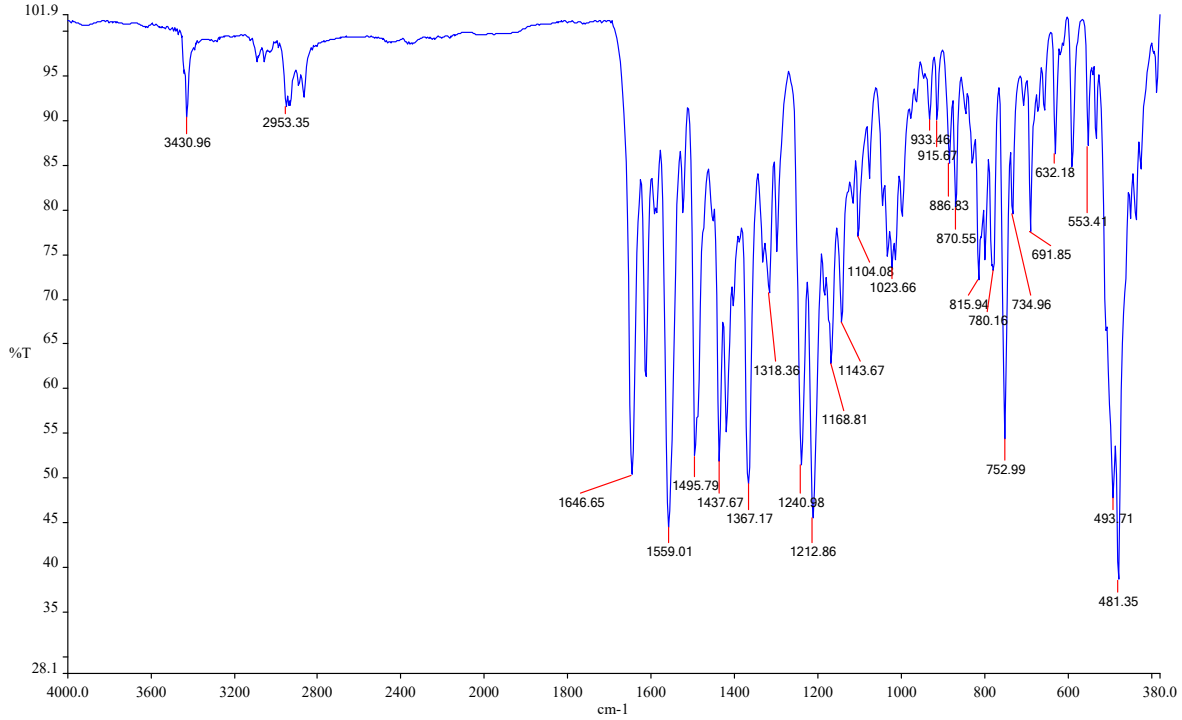

Figure S20: IR spectrum of **3j**

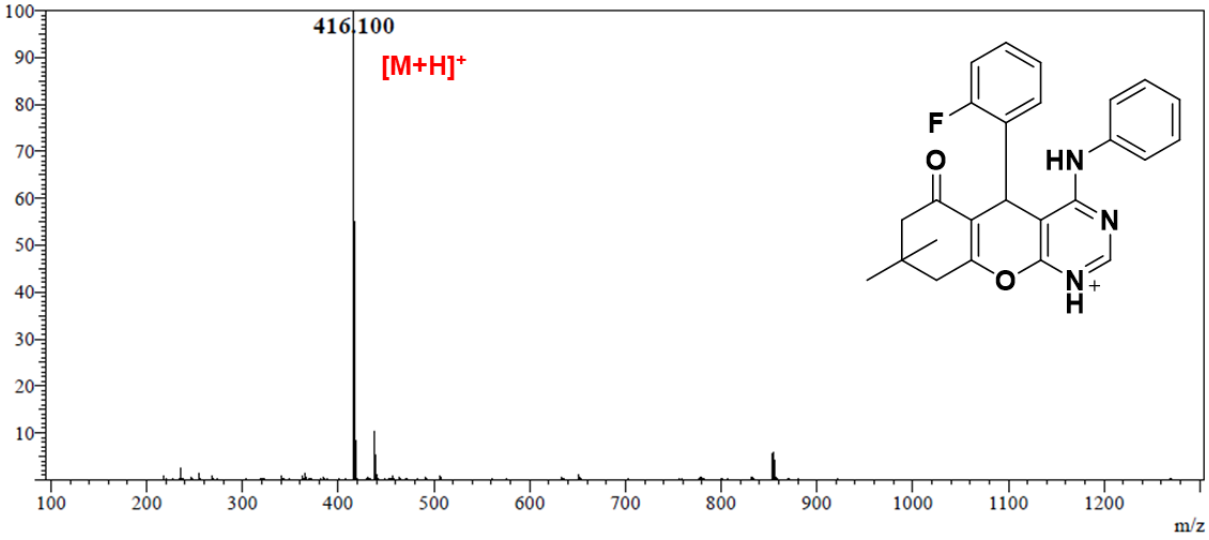

Figure S21: ESI(+)MS of **3a**

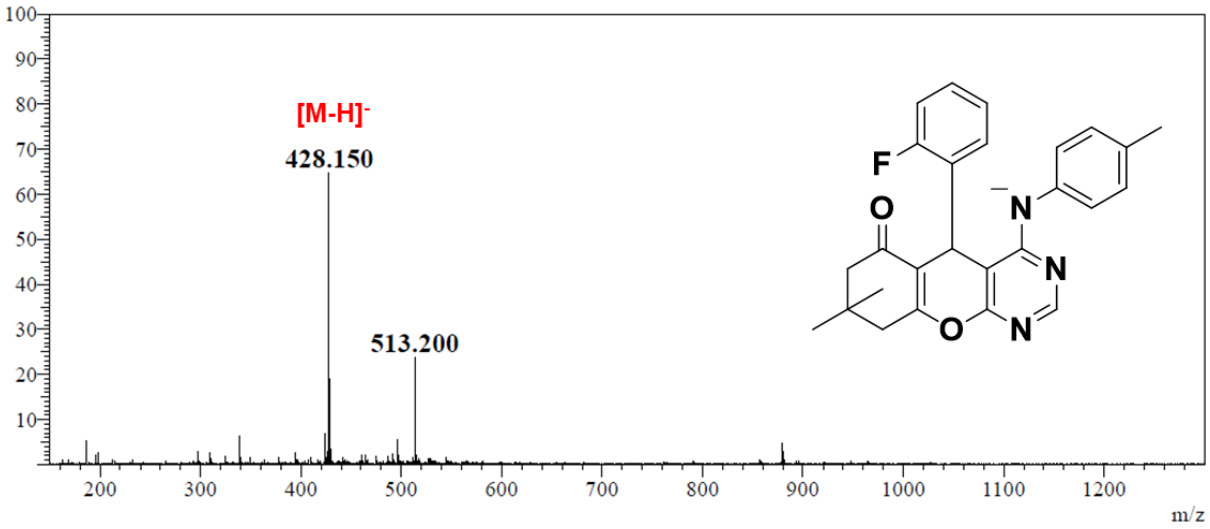

Figure S22: ESI(-)MS of **3b**

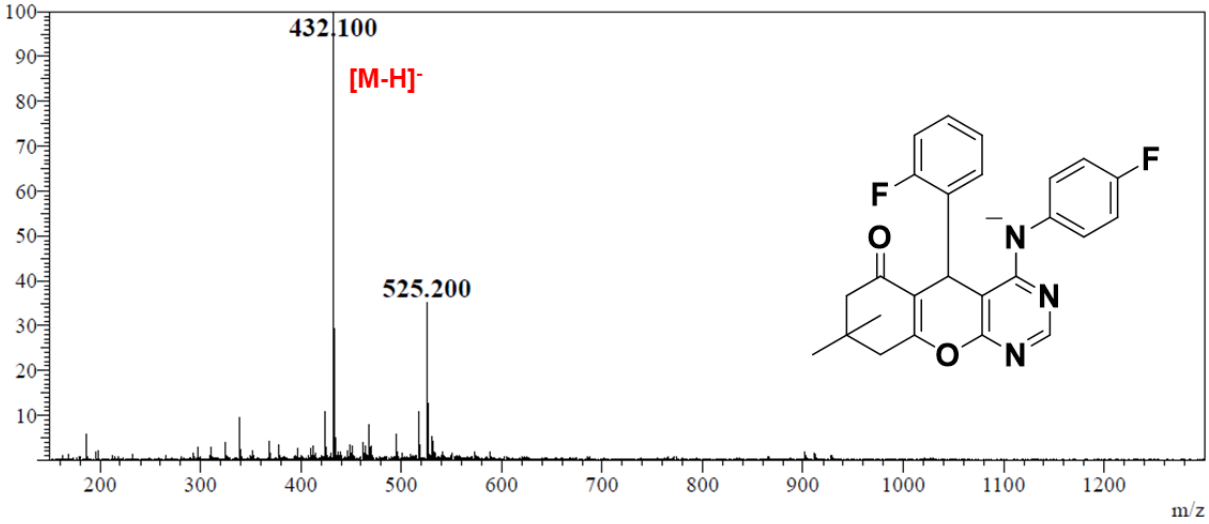

Figure S23: ESI(-)MS of **3c**

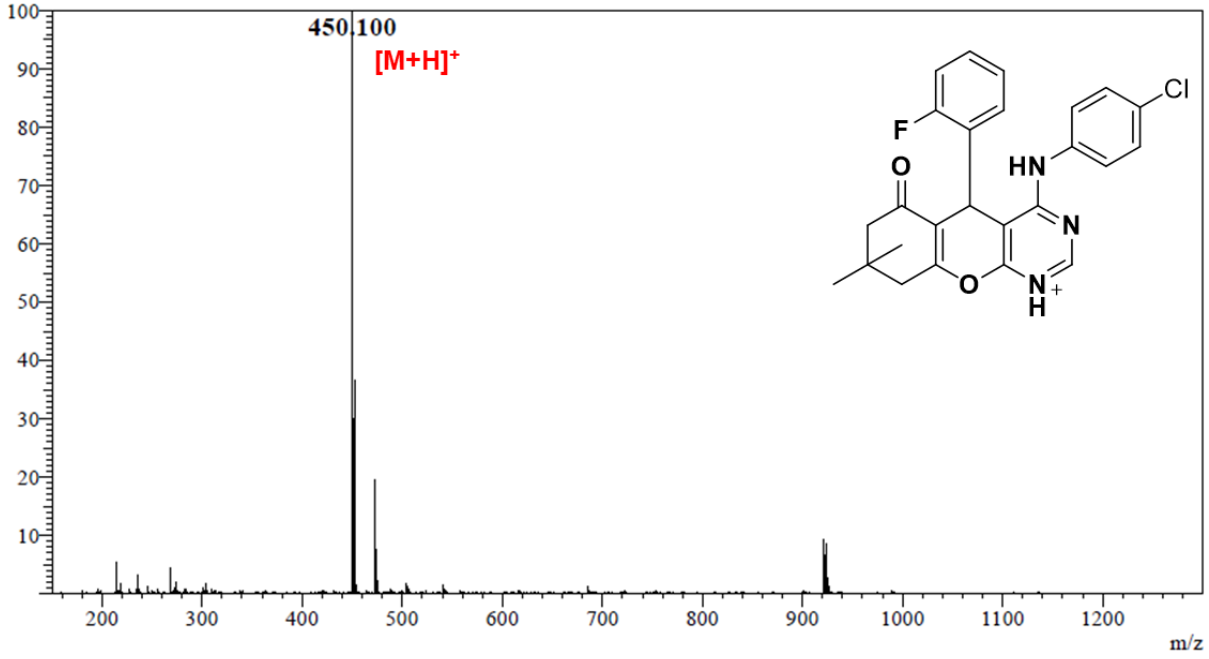

Figure S24: ESI(-)MS of **3d**

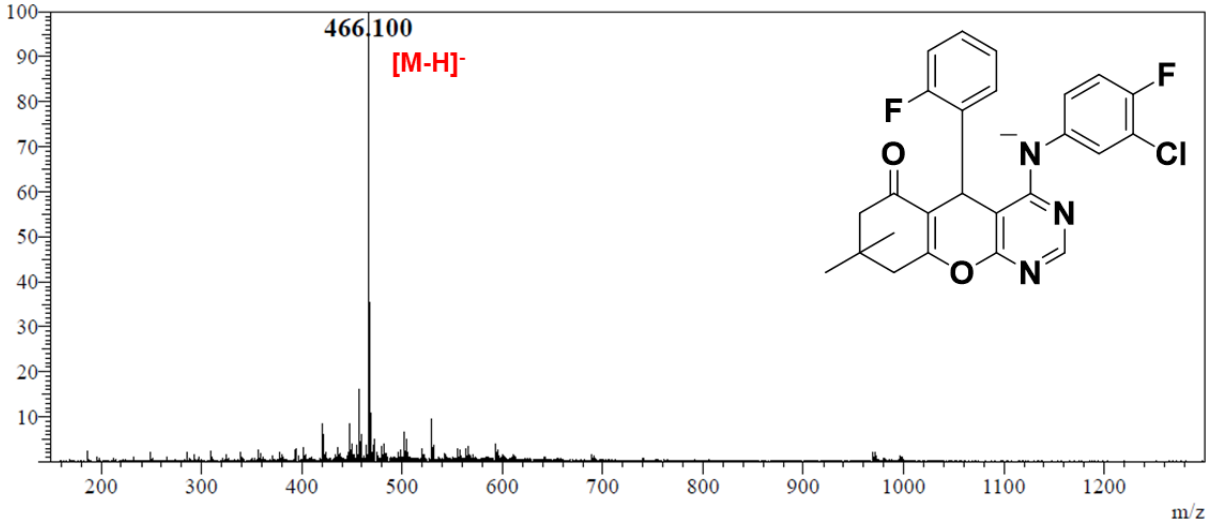

Figure S25: ESI(-)MS of **3e**

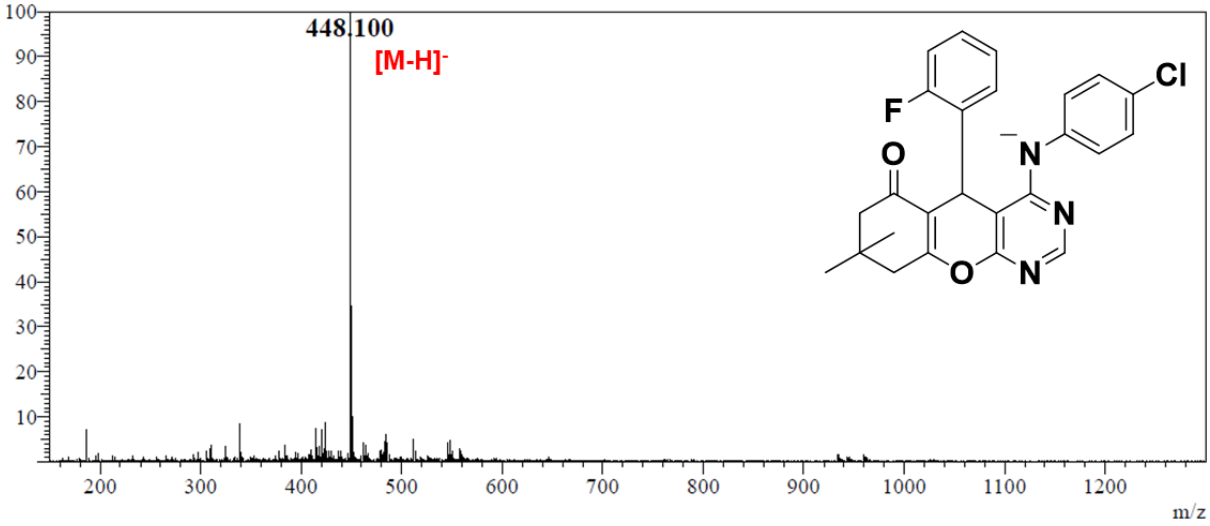

Figure S26: ESI(-)MS of **3f**

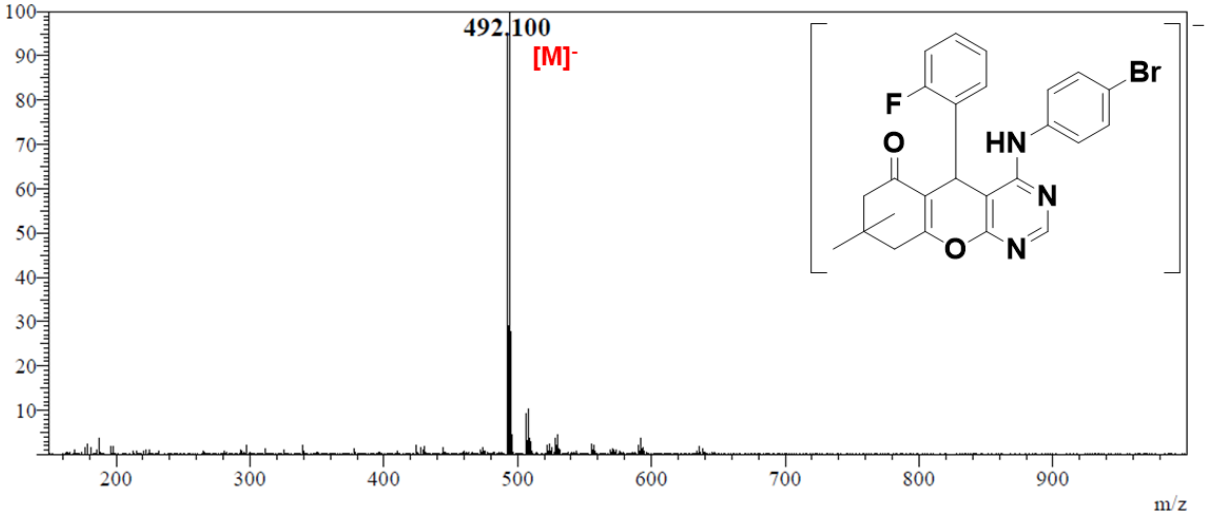

Figure S27: ESI(-)MS of **3g**

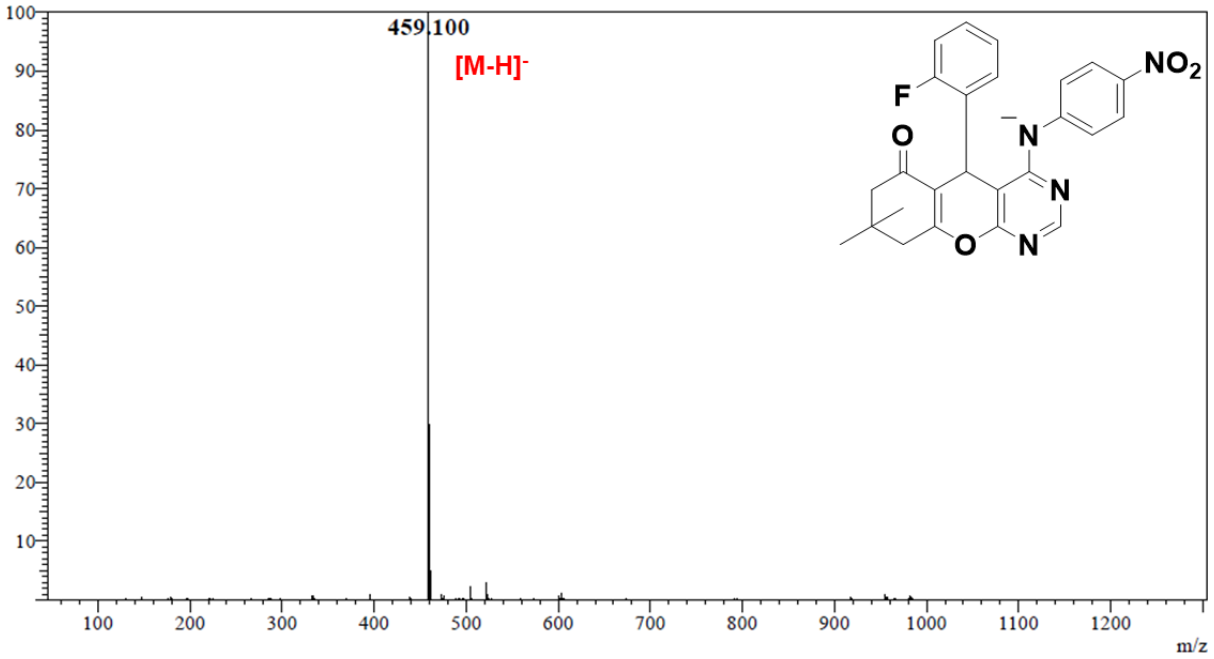

Figure S28: ESI(-)MS of **3h**

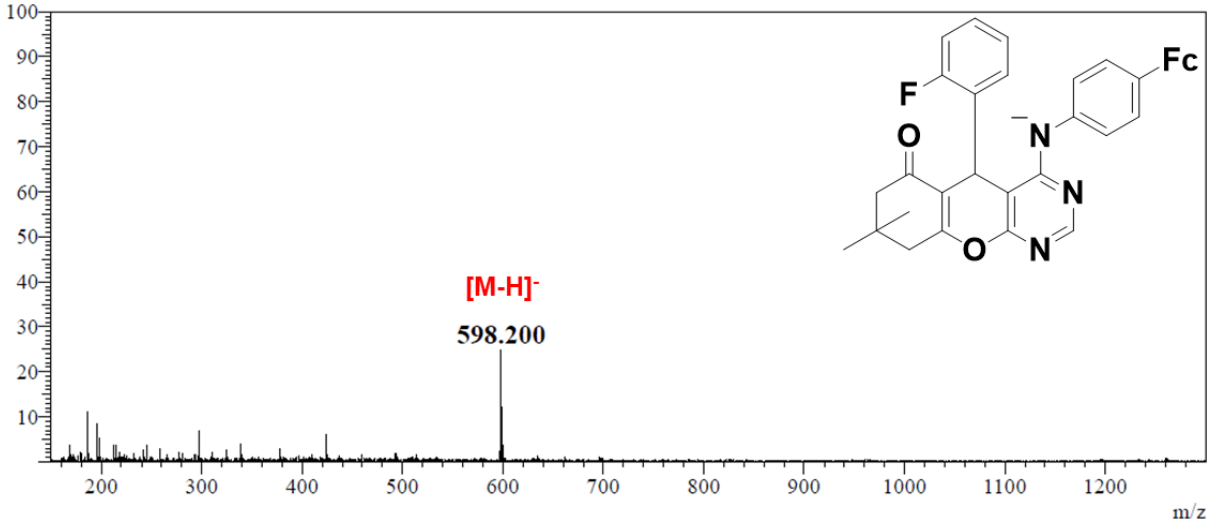

Figure S29: ESI(-)MS of **3i**

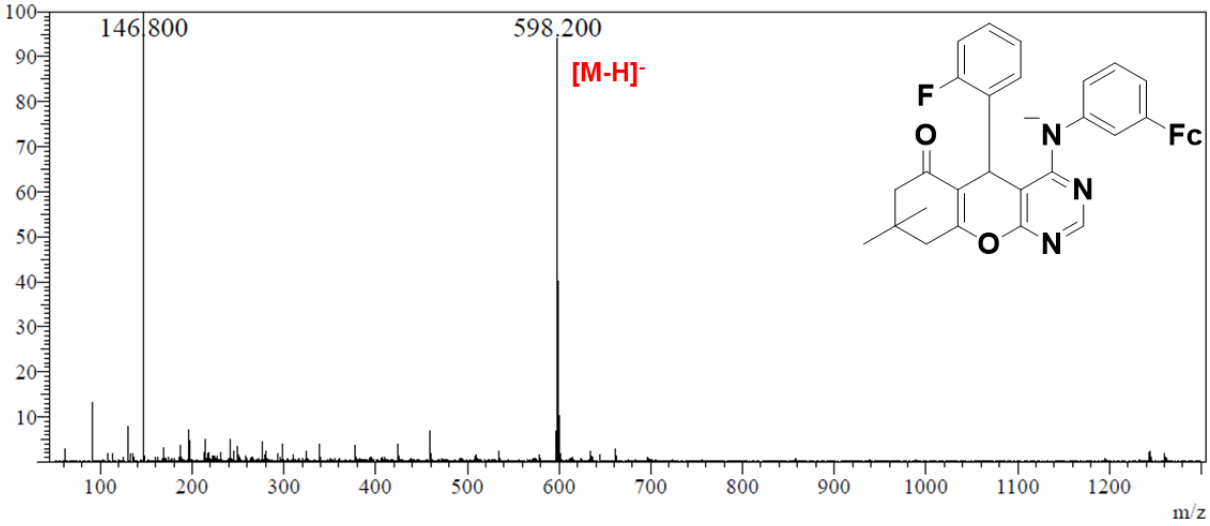

Figure S30: ESI(-)MS of **3j**

Table S1: Selected chemical shifts observed in the ^{1}H NMR spectra of chromenopyrimidines and pK_a values of the corresponding aniline precursor used.

Compound	^{1}H NMR		pK$_a$
	δ_{NH}/ppm	δ_{CH} /ppm	
3a	8.49	8.3	4.61[a]
3b	8.37	8.27	5.04[a]
3c	8.55	8.28	4.66[a]
3d	8.6	8.31	3.54[a]
3e	8.72	8.36	3.60[a]
3f	8.64	8.33	3.97[a]
3g	8.64	8.33	3.90[a]
3h	9.2	8.45	1.01[a]
3i	8.46	8.31	4.78[b]
3j	8.44	8.33	4.88[b]

[a] Calculated using Advanced Chemistry Development (ACD/Labs), Software V11. 02 (1994–2013 ACD/Labs)
[b] Calculated from trendline equation of pK_a *versus* δ_{NH} in Figure 1b

Representation of some hydrogen bonding patterns observed in the crystal packing of **3a**, **3b**, **3c**, **3e**, **3h** and **3j**

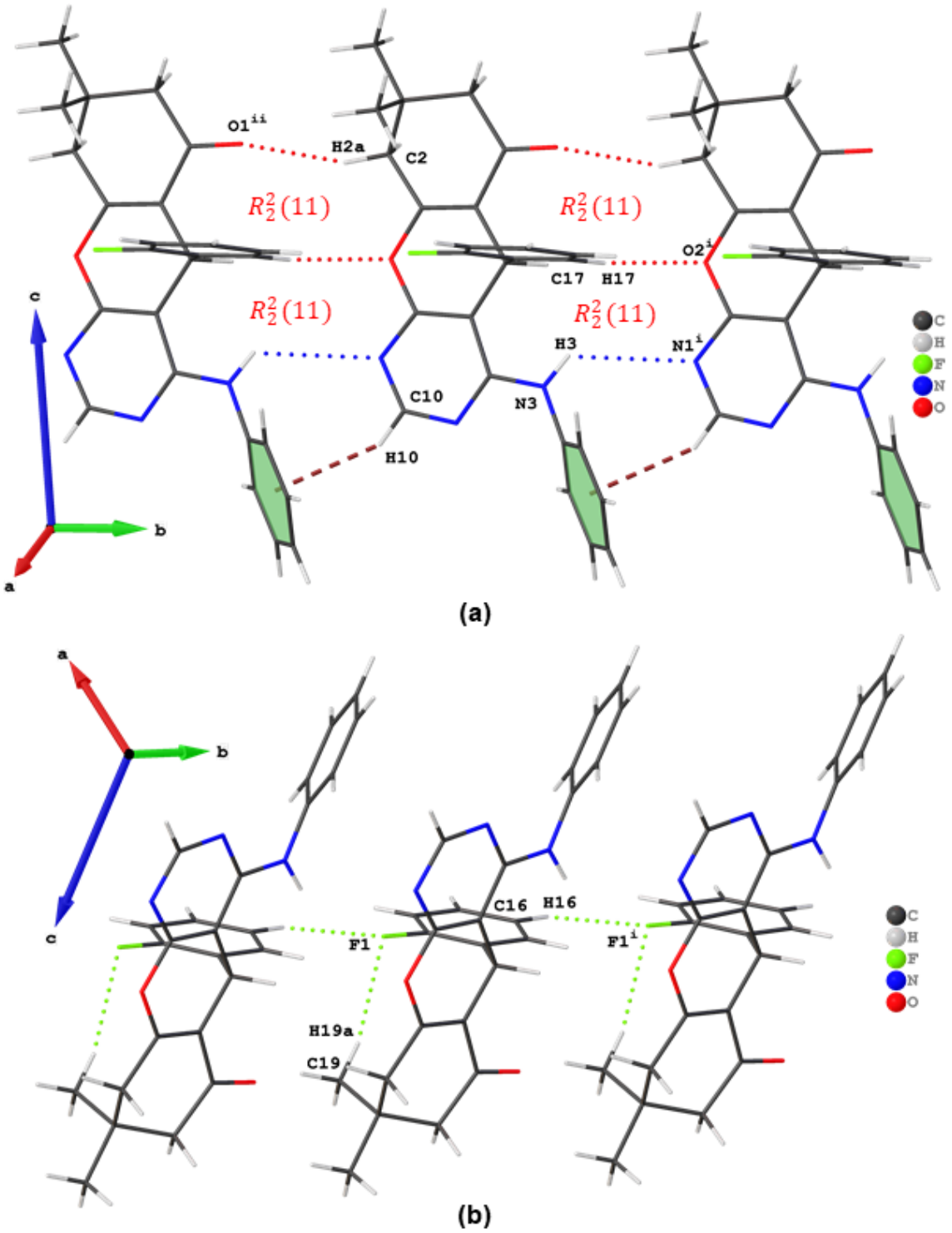

Figure S31: Representation of (a) intermolecular N—H…N, C—H…O, C—H…pi, and (b) C—H…F hydrogen bonding patterns in the crystal packing of **3a** to **3c**. The N—H…N, C—H…O, C—H…pi, and C—H…F interactions are drawn as dotted blue, red, brown and green bonds, respectively. The graphset descriptors that form ring motifs are shown in red text

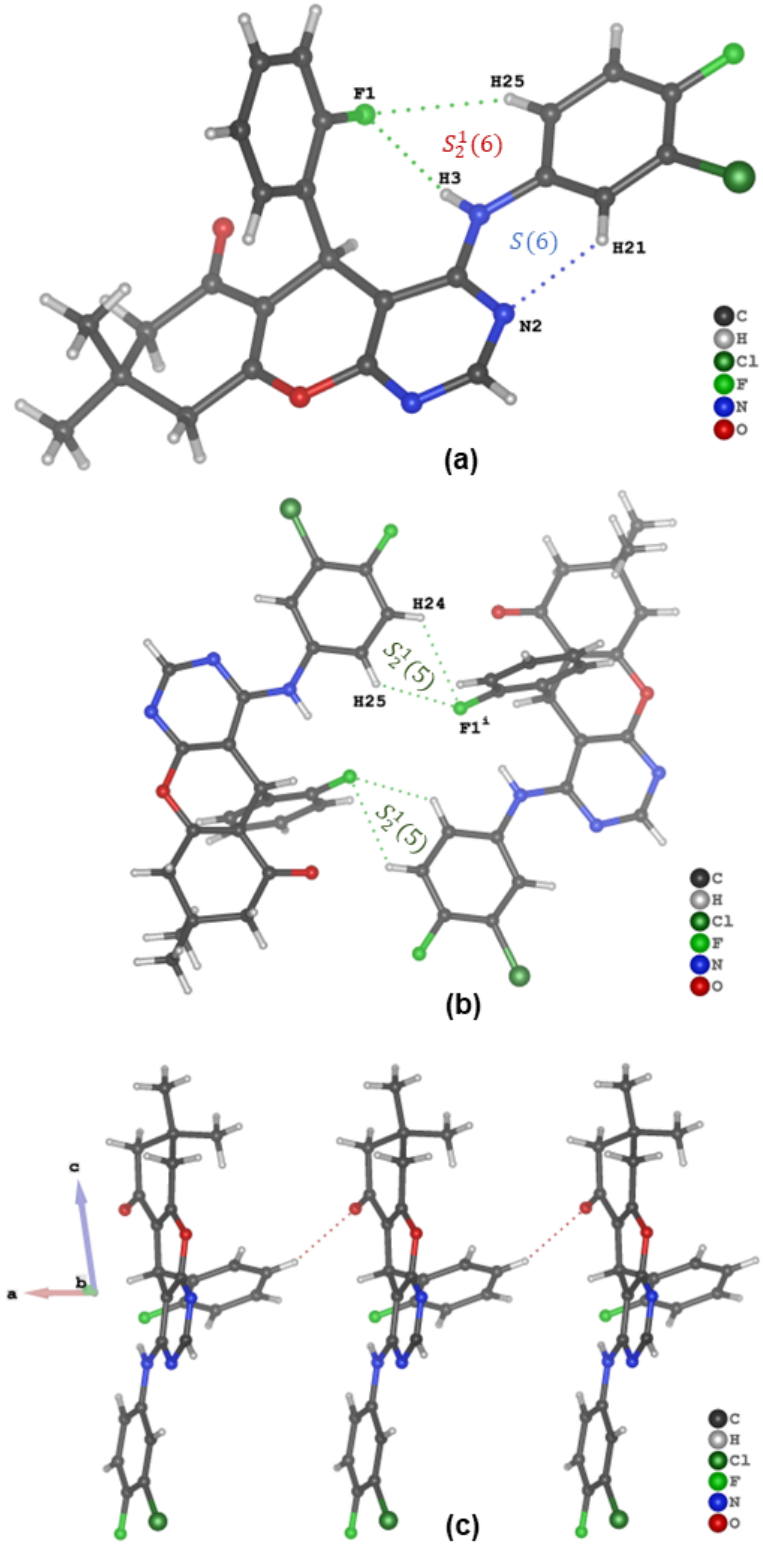

Figure S32: Representation of (a) intramolecular C—H…N, C—H…F, N—H…F, and intermolecular (b) C—H…F and (c) C—H…O hydrogen bonding patterns in the crystal packing of **3e**. The C—…N, C—H…O and C—H…F interactions are drawn as dotted blue, red and green bonds, respectively. The graphset descriptors that form ring motifs are shown in red, blue and green text

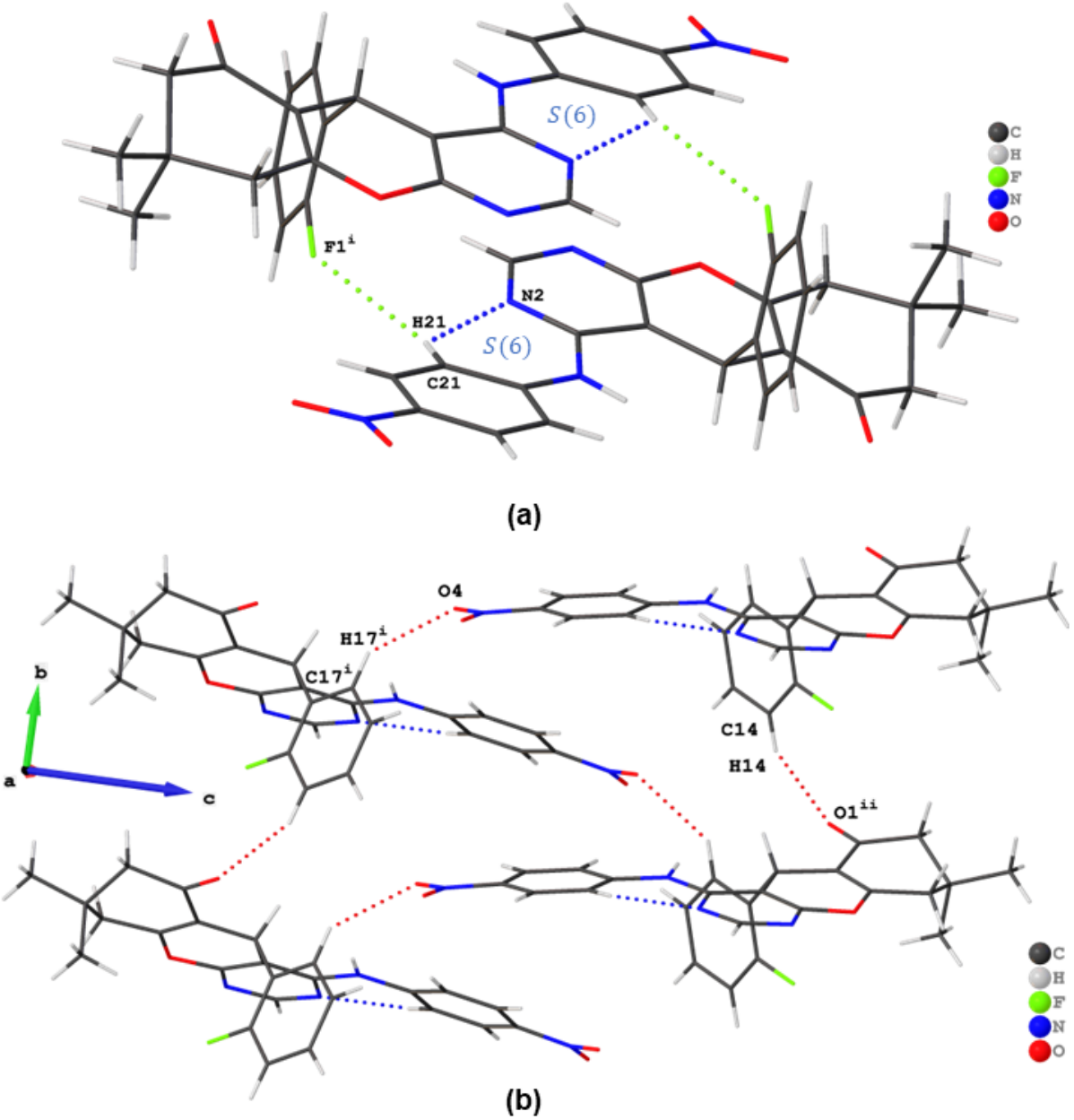

Figure S33: Representation of (a) intramolecular C—H…N, intermolecular C—H…F and (b) C—H…O hydrogen bonding patterns in the crystal packing of **3h**. The C—H…N, C—H…O and C—H…F interactions are drawn as dotted blue, red and green bonds, respectively. The graphset descriptors that form ring motifs are shown in blue text

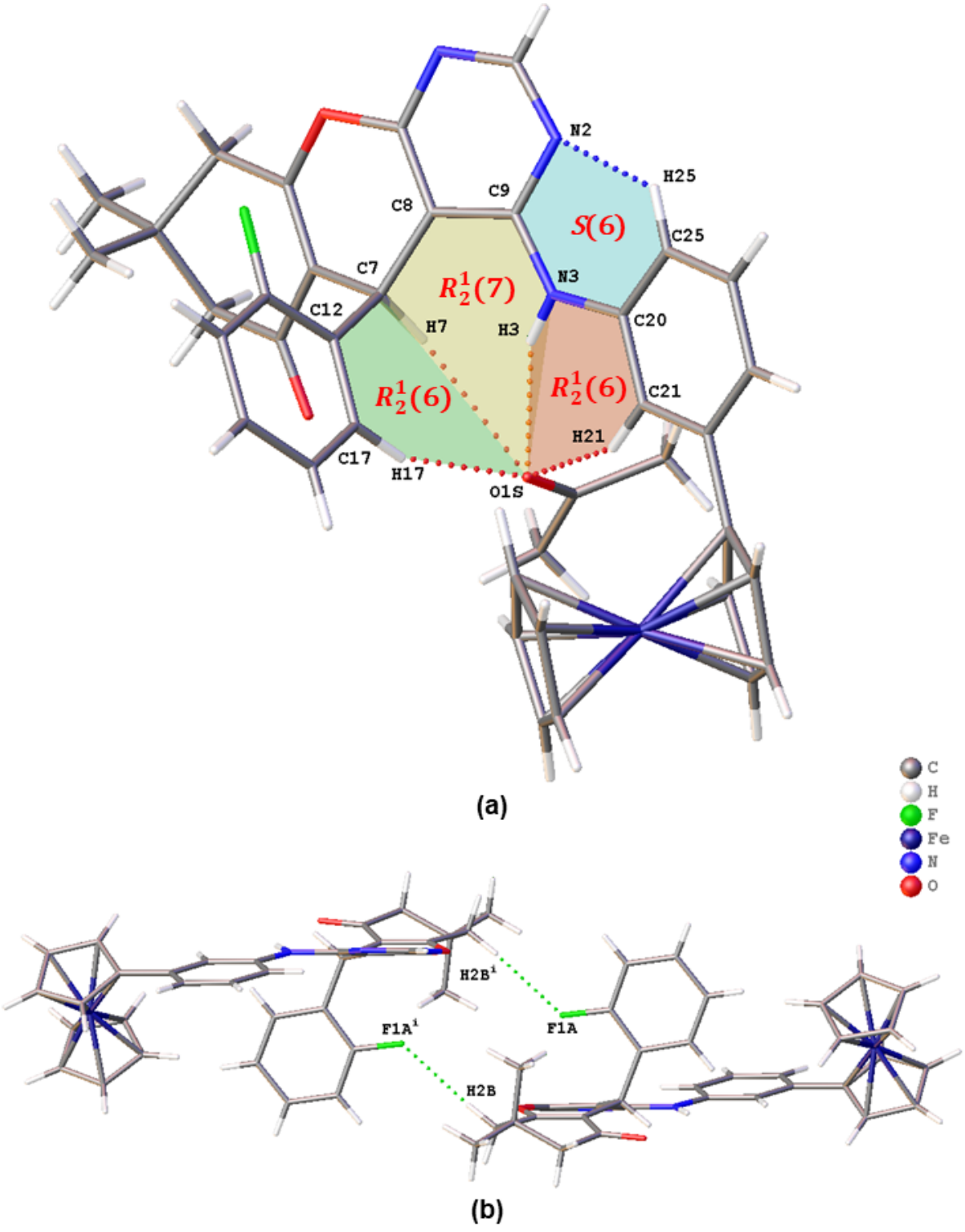

Figure S34: Representation of (a) intramolecular C—H…N, intermolecular N—H…O, C—H…O and (b) C—H…F hydrogen bonding patterns in the crystal packing of **3j**. The C—H…N, N—H…O, C—H…O and C—H…F interactions are drawn as dotted blue, orange, red and green bonds, respectively. The graphset descriptors that form ring motifs are shown in red text

Table S2: Geometric parameters of selected hydrogen bonding patterns in **3a** to **3c**, **3e**, **3h** and **3j**

D-H…A	d(D-H)/Å	d(H…A)/Å	d(D…A)/Å	D-H…A/°
Compound 3a				
C2-H2A…O1^{i}	0.99	2.42	3.354(2)	156
C16-H16…F1^{ii}	0.95	2.49	3.372(2)	155
C17-H17…O2^{ii}	0.95	2.47	3.397(2)	165
Compound 3b				
C2-H2A…N1^{i}	0.99	2.63	3.458(2)	142
C2-H2B…O1^{ii}	0.99	2.46	3.383(2)	155
C18-H18…F1^{iii}	0.95	2.52	3.410(2)	155
C19-H19…O2^{iii}	0.95	2.49	3.414(2)	165
Compound 3c				
C2-H2A…O1^{i}	0.99	2.42	3.353(1)	156
C18-H18…F1^{ii}	0.95	2.49	3.369(1)	154
C19-H19…O2^{ii}	0.95	2.48	3.406(1)	166
Compound 3e				
N3-H3…F1	0.88	2.22	3.059(2)	159
C16-H16…O1^{i}	0.95	2.55	3.451(2)	159
C21-H21…N2	0.95	2.26	2.887(2)	122
C24-H24…F1^{ii}	0.95	2.77	3.363(2)	121
C25-H25…F1	0.95	2.69	3.452(2)	138
C25-H25…F1^{ii}	0.95	2.68	3.327(2)	126
Compound 3h				
C21-H21…F1^{i}	0.95	2.45	3.071(2)	123
C21-H21…N2	0.95	2.25	2.866(2)	122
C14-H14…O1^{ii}	0.95	2.27	3.144(2)	152
C17-H17…O4^{iii}	0.95	2.45	3.244(2)	141
Compound 3j				
C21—H21…O1S	0.95	2.55	3.387(2)	147
N3—H3…O1S	0.88	2.38	3.215(2)	159
C7—H7…O1S	0.99	2.60	3.520(2)	153
C17—H17…O1S	0.95	2.37	3.264(3)	157
C2—H2B…F1A^{i}	0.99	2.57	3.508(2)	158
C25—H25…N2	0.95	2.26	2.875(2)	122

Symmetry codes: **3a** (i) *x*,-1+*y*,*z*; (ii) *x*,-1+*y*,*z*; **3b** (i) (i) *x*,-1+*y*,*z*; (ii) *x*,-1+*y*,*z*; **3c** (i) (i) *x*,-1+*y*,*z*; (ii) *x*,-1+*y*,*z;* **3e** (i) -1+*x*,*y*,*z*; (ii) 1-*x*,1-*y*,1-*z*; **3h** (i) 3/2-*x*,-1/2-*y*,-*Z*; (ii) *x*,-1+*y*,*z*; (iii) 3/2-*x*,1/2+*y*,-1/2-*z*; **3j** (i) 2-*x*,-*y*,-*z*

Table S3: Crystallographic data and structural refinement details for **3a** to **3c, 3e, 3h** and **3j**

	3a	**3b**	**3c**	**3e**	**3h**	**3j**
Chemical formula	$C_{25}H_{22}FN_3O_2$	$C_{26}H_{24}FN_3O_2$	$C_{25}H_{21}F_2N_3O_2$	$C_{25}H_{20}ClF_2N_3O_2$	$C_{25}H_{21}FN_4O_4$	$C_{35}H_{30}FFeN_3O_2 \cdot C_3H_6O$
M_r	415.45	429.48	433.45	467.89	460.46	657.55
Crystal system, space group	Monoclinic, $P2_1/c$	Monoclinic, $P2_1/c$	Monoclinic, $P2_1/c$	Triclinic, $P\bar{1}$	Monoclinic, $I2/c$	Monoclinic, $P2_1/n$
Temperature (K)	100	100	100	100	100	150
a, b, c (Å)	12.0927 (4), 7.3784 (2), 21.8294 (7)	12.1596 (4), 7.4148 (3), 23.0902 (9)	12.1368 (3), 7.3737 (2), 22.1506 (5)	7.2220 (1), 10.4778 (2), 14.4403 (3)	21.5323 (4), 6.9303 (1), 29.2911 (7)	11.1910 (3), 10.9002 (3), 25.9816 (8)
α, β, γ (°)	90, 93.390 (2), 90	90, 96.662 (2), 90	90, 94.506 (1), 90	75.338 (1), 82.465 (1), 85.928 (1)	90, 93.555 (1), 90	90, 97.846 (2), 90
V (Å^3)	1944.32 (10)	2067.78 (13)	1976.20 (9)	1047.18 (3)	4362.56 (15)	3139.67 (16)
Z	4	4	4	2	8	4
μ (mm^{-1})	0.10	0.10	0.11	0.23	0.10	0.53
Crystal size (mm)	0.34 × 0.21 × 0.14	0.27 × 0.15 × 0.11	0.39 × 0.37 × 0.32	0.36 × 0.31 × 0.24	0.27 × 0.22 × 0.13	0.22 × 0.19 × 0.14
T_{min}, T_{max}	0.955, 0.998	0.964, 0.998	0.951, 0.978	0.910, 0.957	0.652, 0.746	0.882, 0.940
No. of measured, independent and observed [$I > 2\sigma(I)$] reflections	13125, 3863, 2987	13147, 4230, 3118	32619, 4921, 4579	21374, 5268, 4808	17399, 5402, 4369	22501, 6680, 5505
R_{int}	0.031	0.028	0.020	0.027	0.022	0.025
$(\sin\theta/\lambda)_{max}$ (Å^{-1})	0.627	0.629	0.670	0.675	0.670	0.643
$R[F^2 > 2\sigma(F^2)]$, $wR(F^2)$, S	0.0403, 0.0910, 1.034	0.0423, 0.0909, 1.008	0.0394, 0.1029, 1.042	0.0402, 0.1116, 1.057	0.0358, 0.0897, 1.017	0.0371, 0.0897, 1.035
No. of reflections	3863	4230	4921	5268	5402	6680
$\Delta\rho_{max}$, $\Delta\rho_{min}$ (e Å^{-3})	0.23, −0.41	0.29, −0.24	0.33, −0.36	1.19, −0.37	0.35, −0.23	0.99, −0.36

Electronic absorption spectra: DNA and BSA binding affinity

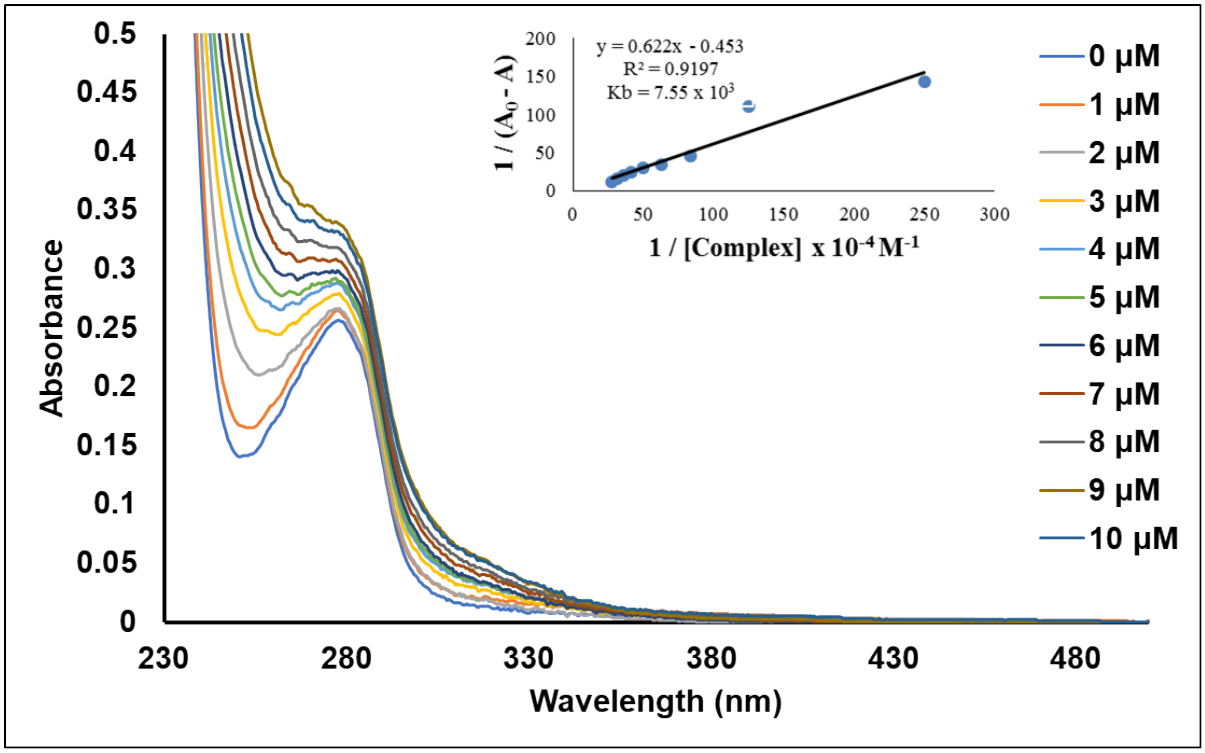

(a)

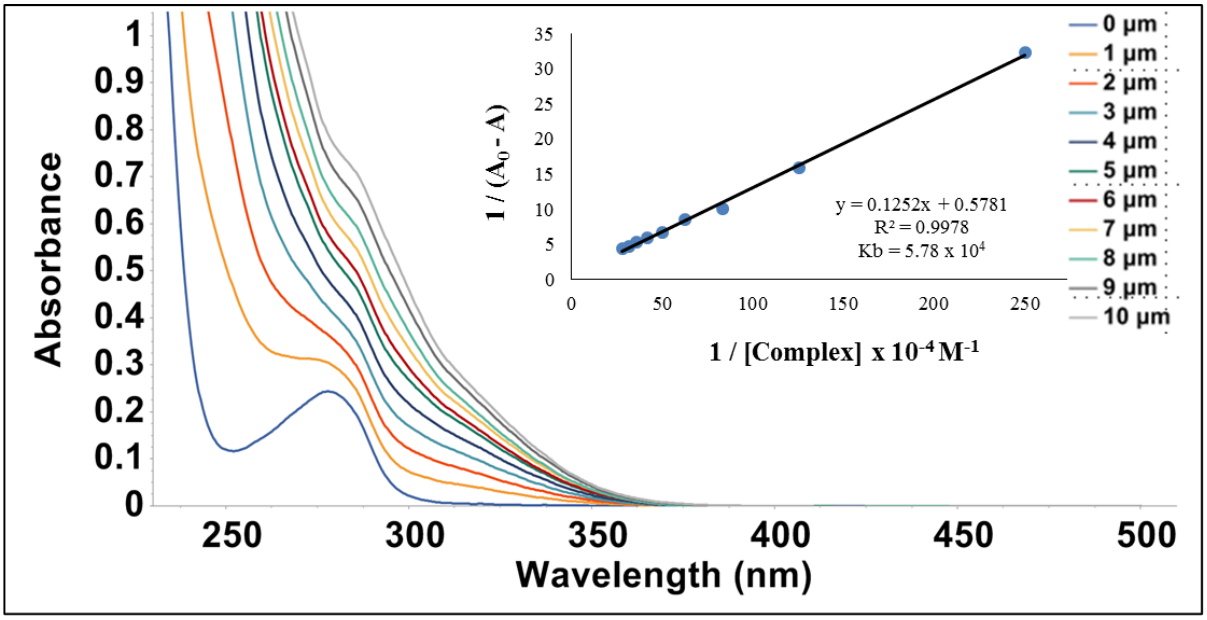

(b)

Figure S35: Absorption spectra of BSA in the absence and presence of increasing amounts of (a) **i-a** and (b) **i-b**.

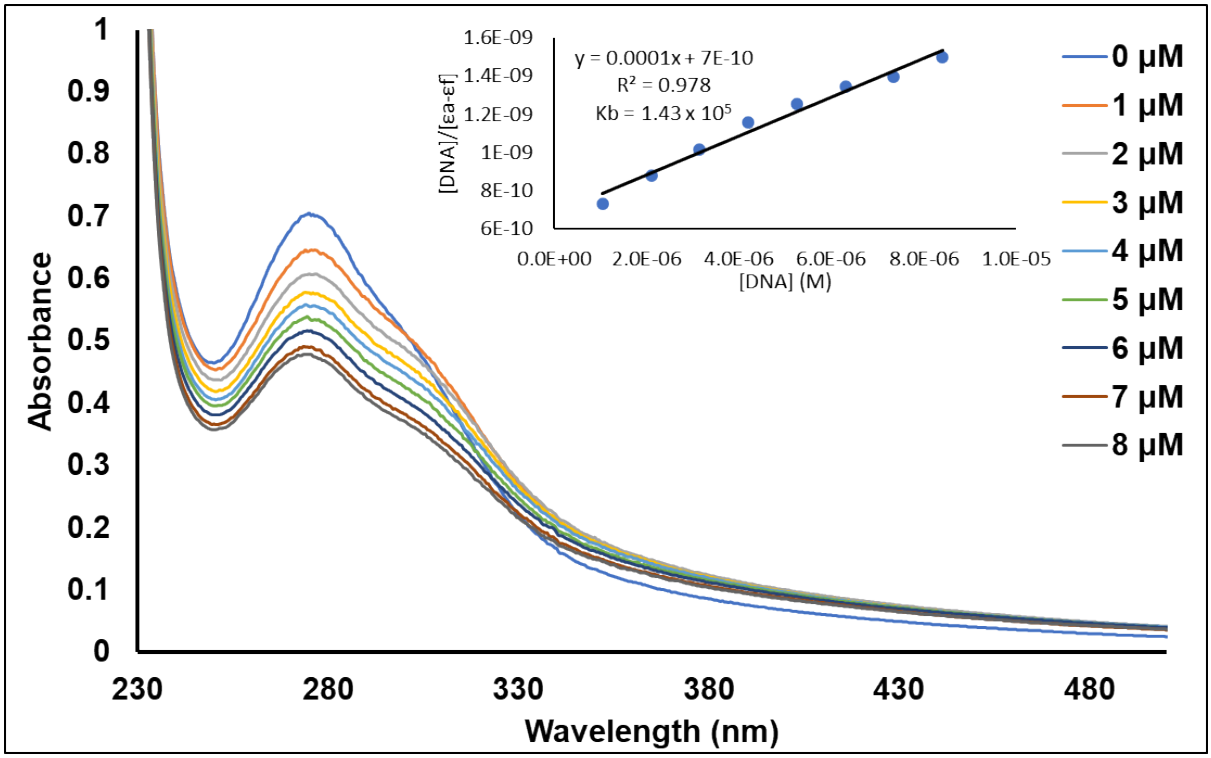

(a)

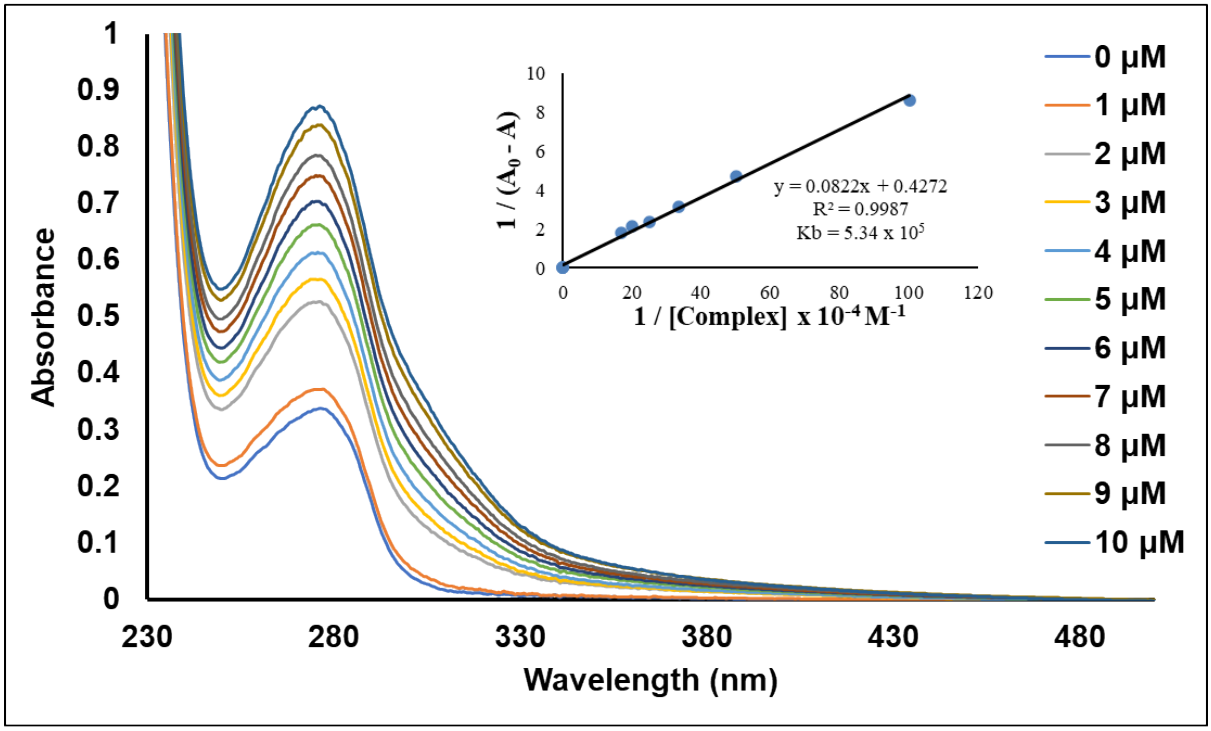

(b)

Figure S36: (a) Absorption spectra of **3a** in the absence and presence of increasing amounts of CT-DNA and (b) absorption spectra of BSA in the absence and presence of increasing amounts of **3a**.

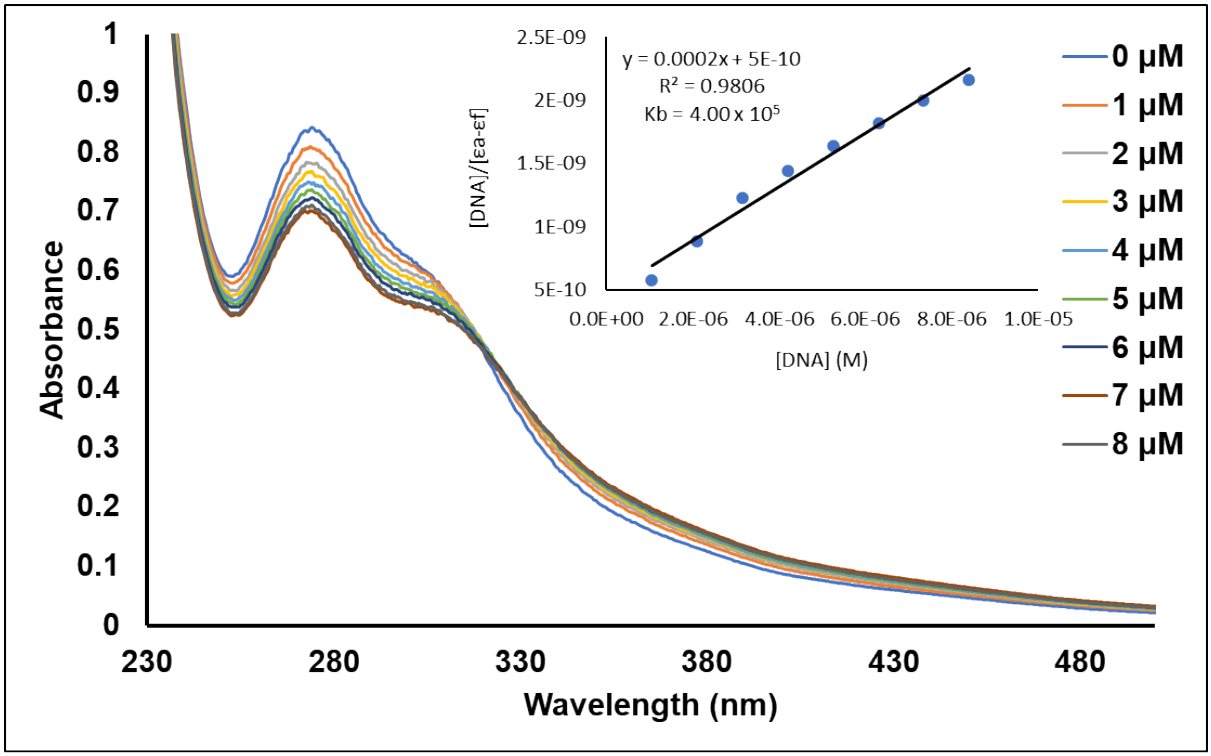

(a)

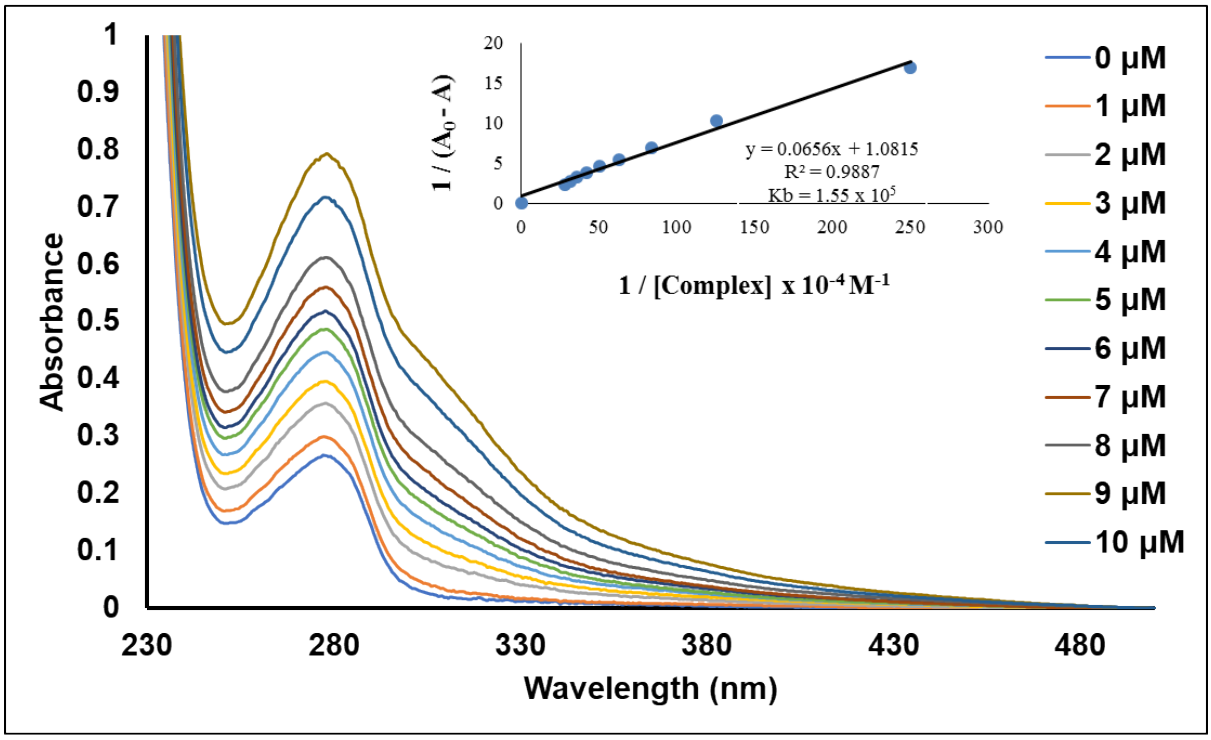

(b)

Figure S37: (a) Absorption spectra of **3b** in the absence and presence of increasing amounts of CT-DNA and (b) absorption spectra of BSA in the absence and presence of increasing amounts of **3b**.

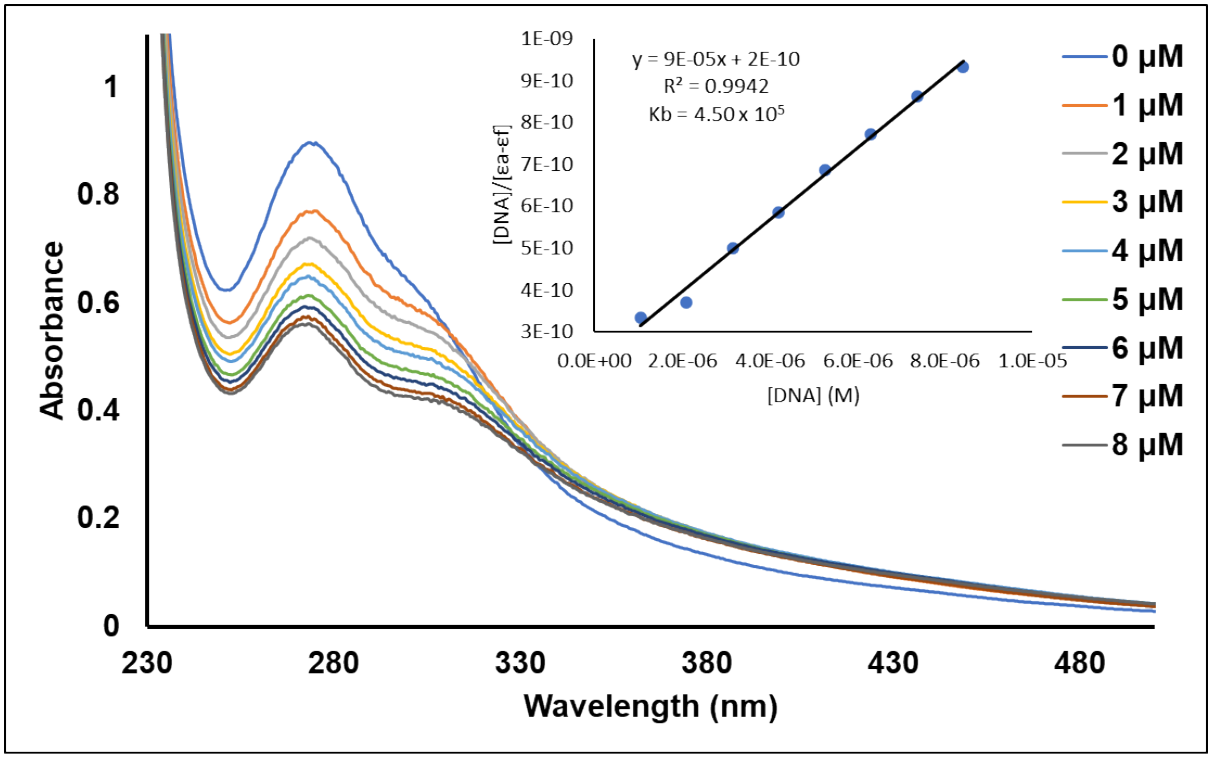

(a)

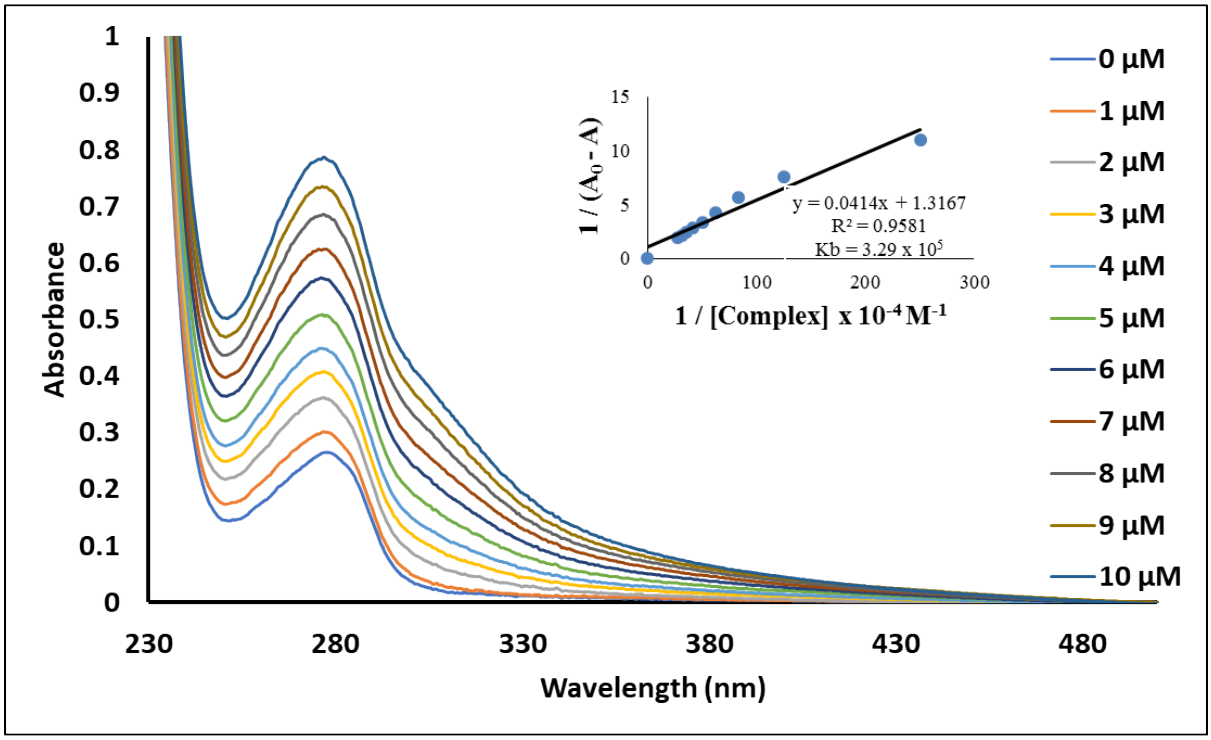

(b)

Figure S38: (a) Absorption spectra of **3c** in the absence and presence of increasing amounts of CT-DNA and (b) absorption spectra of BSA in the absence and presence of increasing amounts of **3c**.

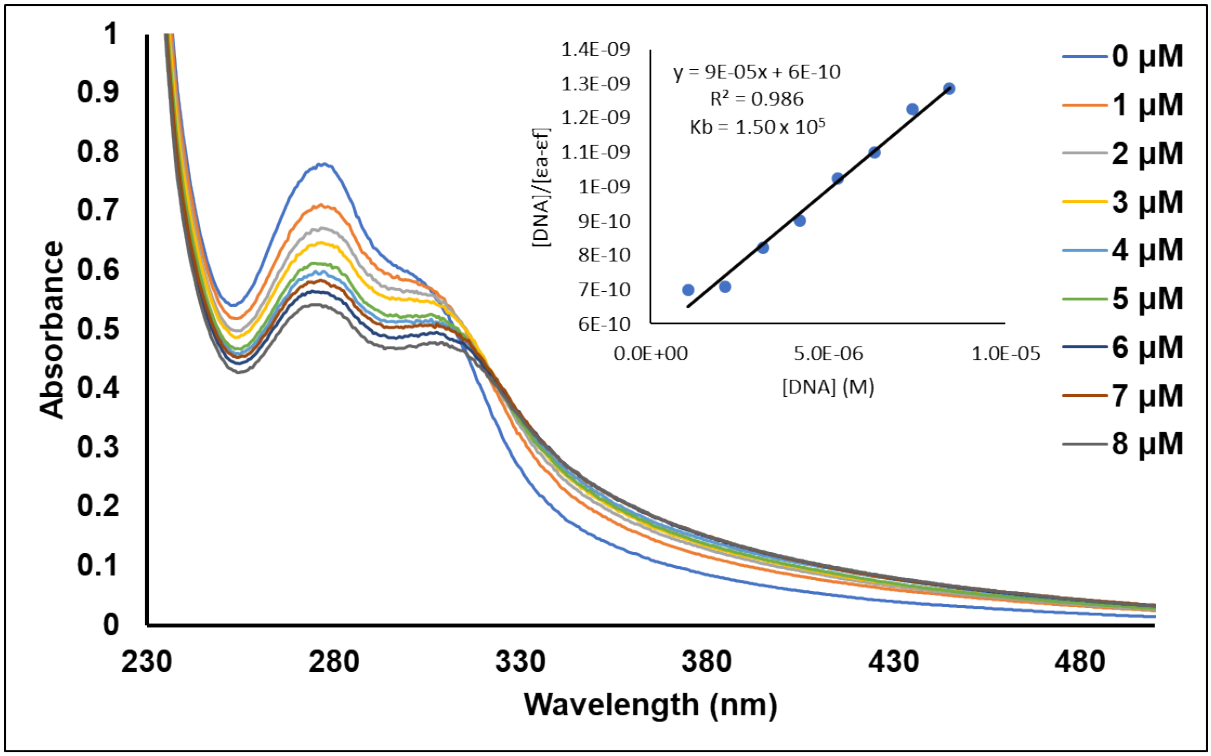

(a)

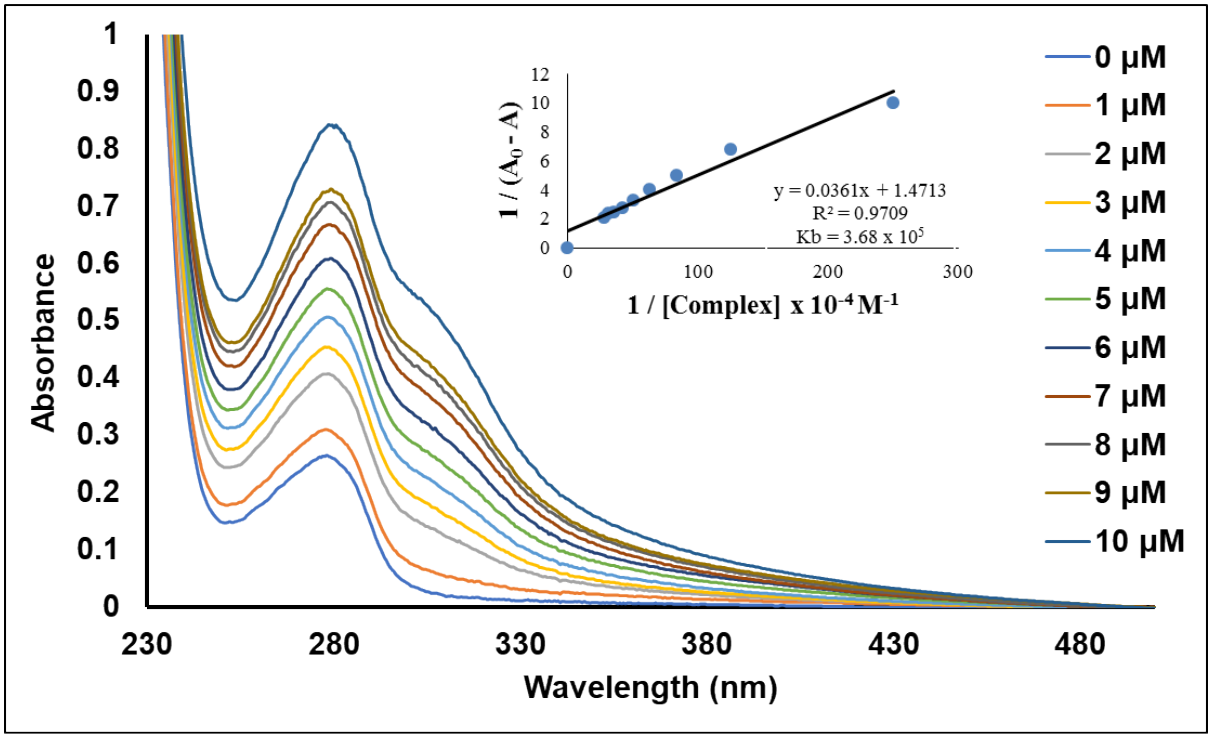

(b)

Figure S39: (a) Absorption spectra of **3d** in the absence and presence of increasing amounts of CT-DNA and (b) absorption spectra of BSA in the absence and presence of increasing amounts of **3d**.

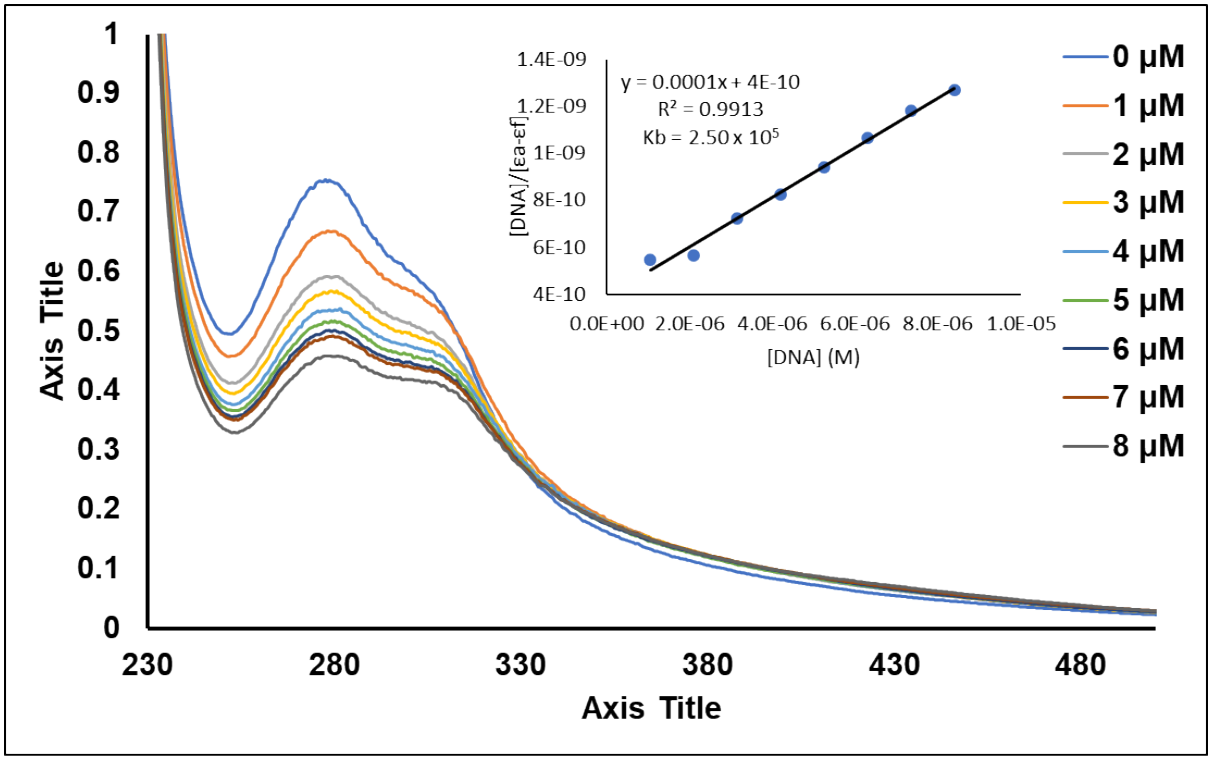

(a)

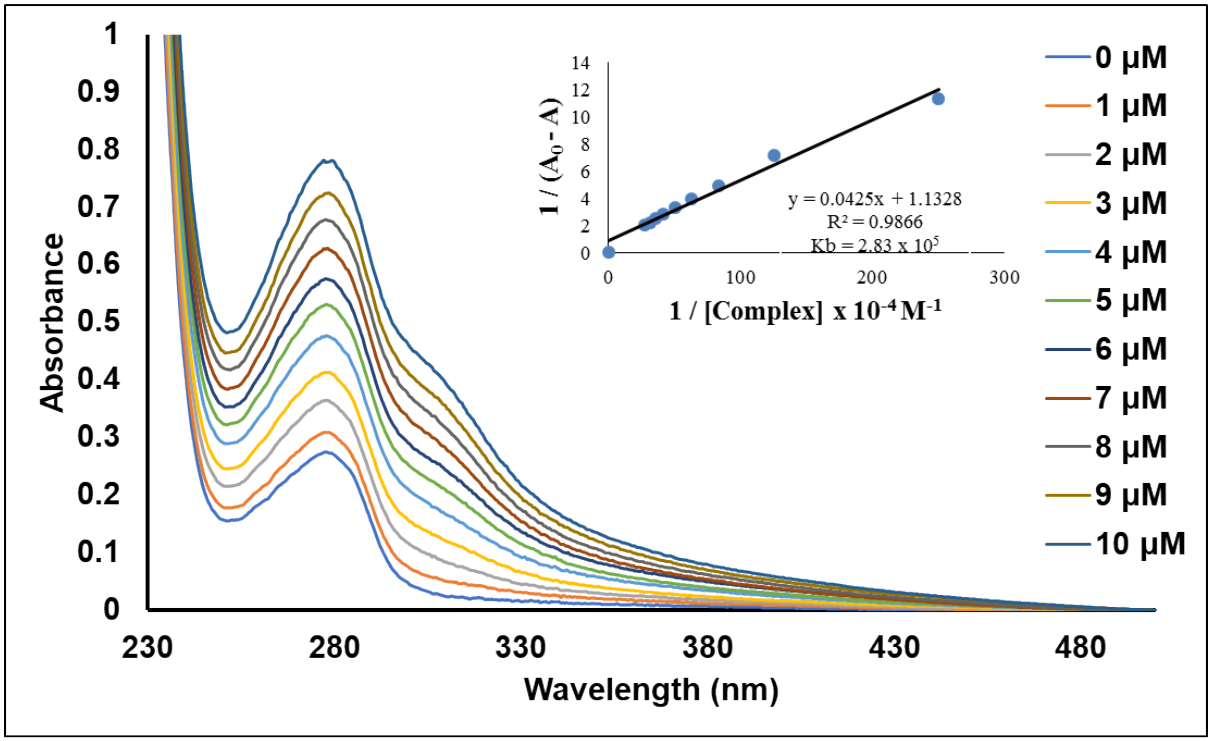

(b)

Figure S40: (a) Absorption spectra of **3e** in the absence and presence of increasing amounts of CT-DNA and (b) absorption spectra of BSA in the absence and presence of increasing amounts of **3e**.

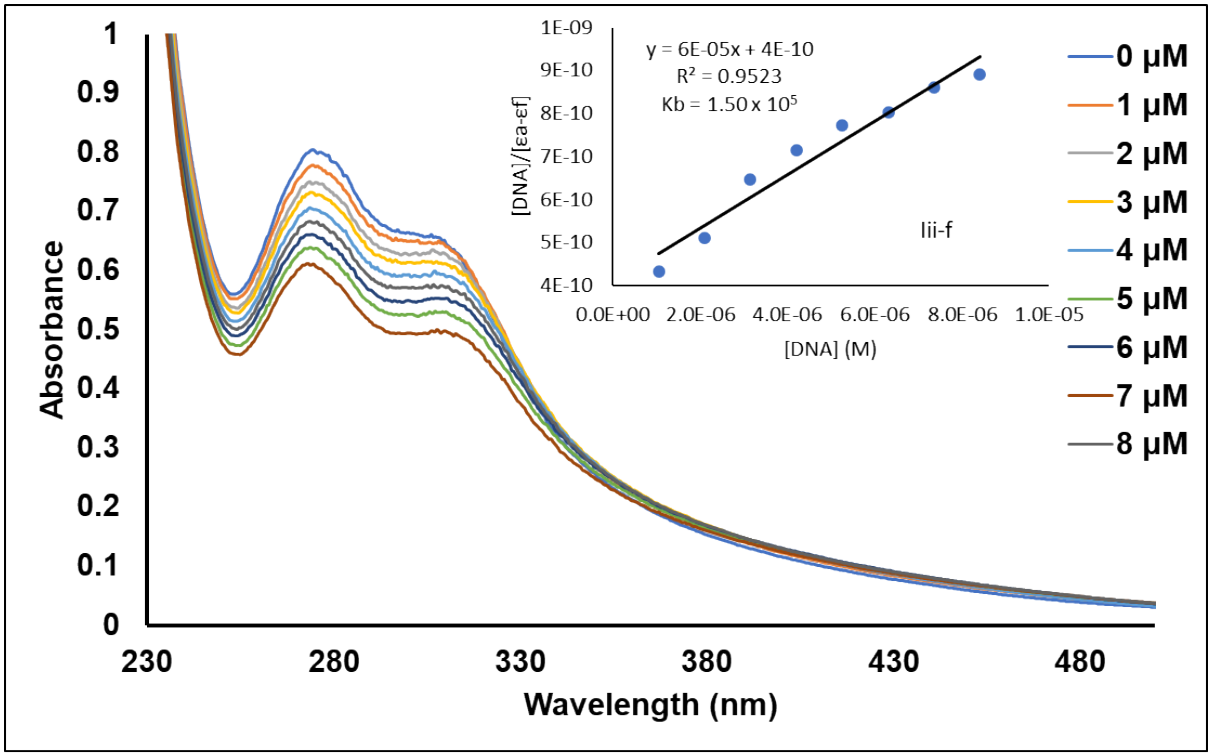

(a)

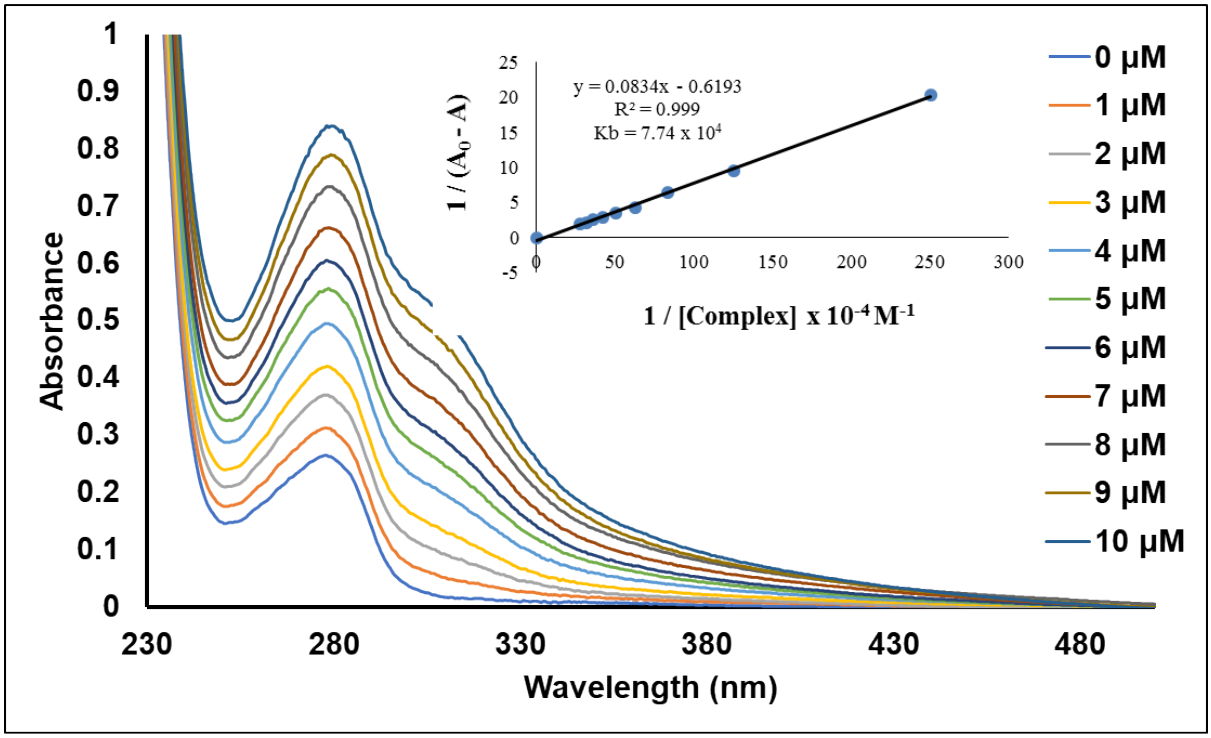

(b)

Figure S41: (a) Absorption spectra of **3f** in the absence and presence of increasing amounts of CT-DNA and (b) absorption spectra of BSA in the absence and presence of increasing amounts of **3f**.

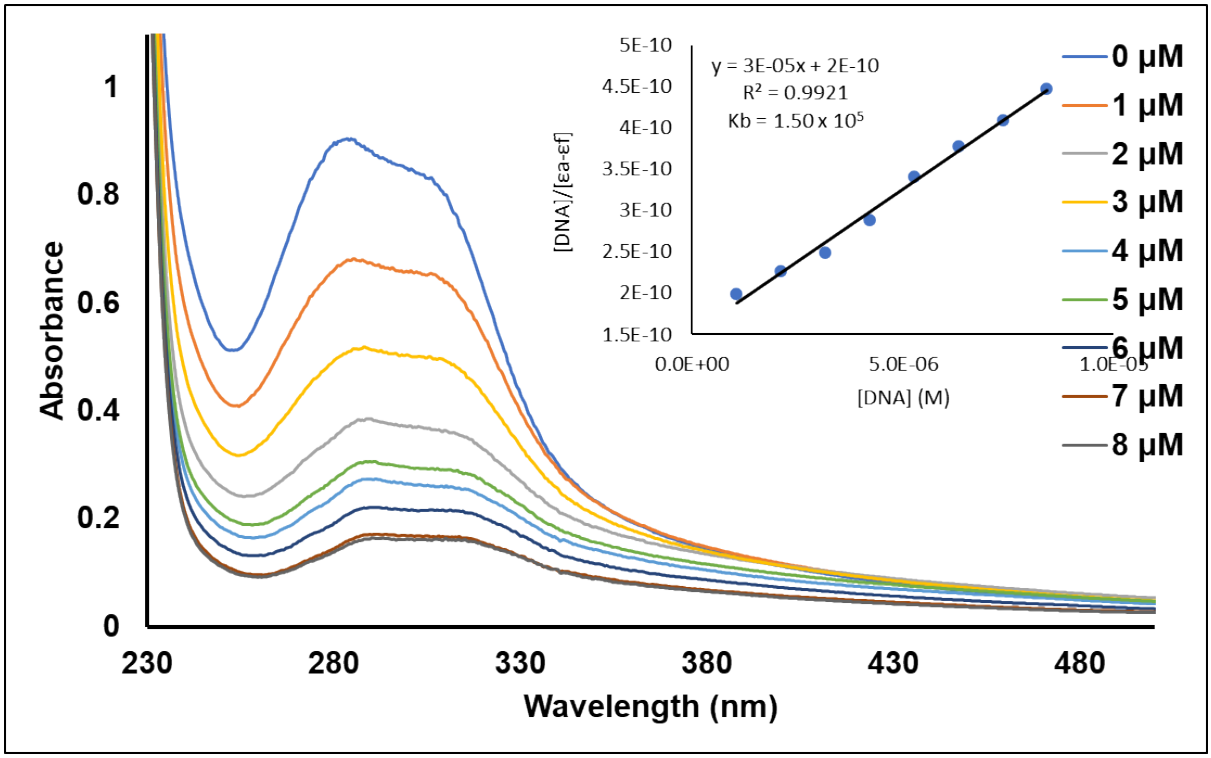

(a)

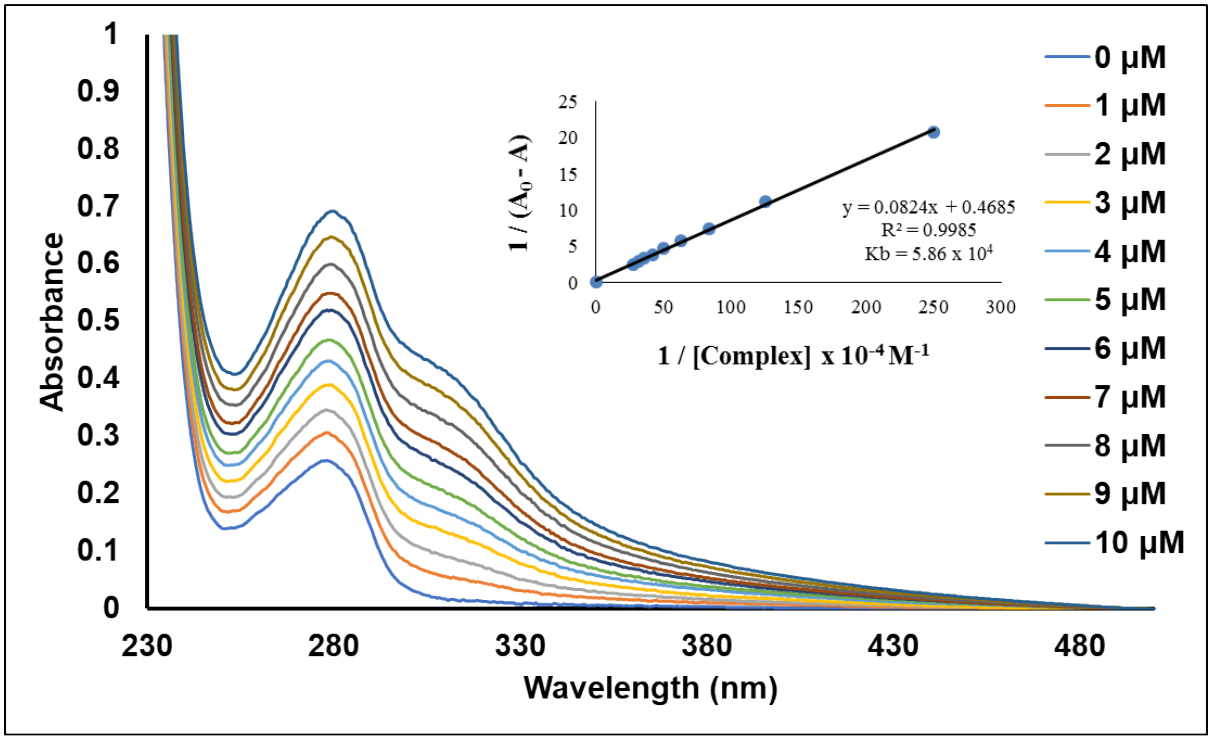

(b)

Figure S42: (a) Absorption spectra of **3g** in the absence and presence of increasing amounts of CT-DNA and (b) absorption spectra of BSA in the absence and presence of increasing amounts of **3g**.

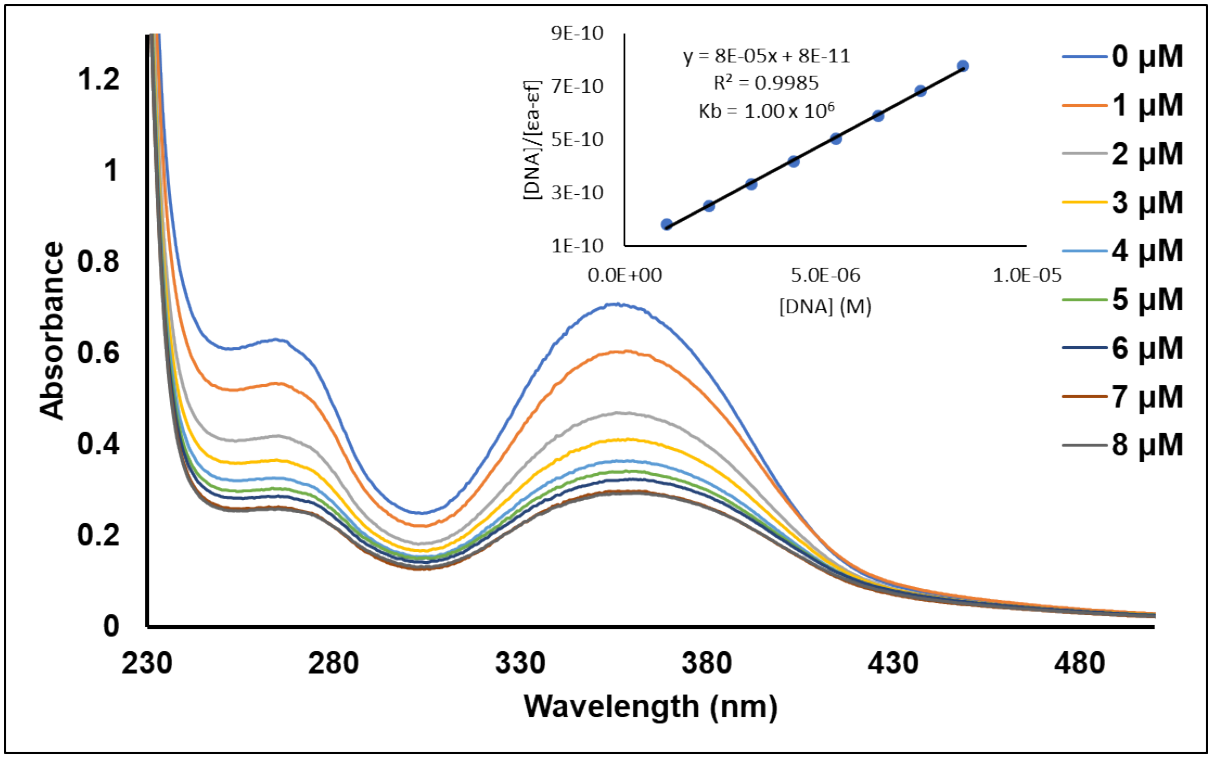

(a)

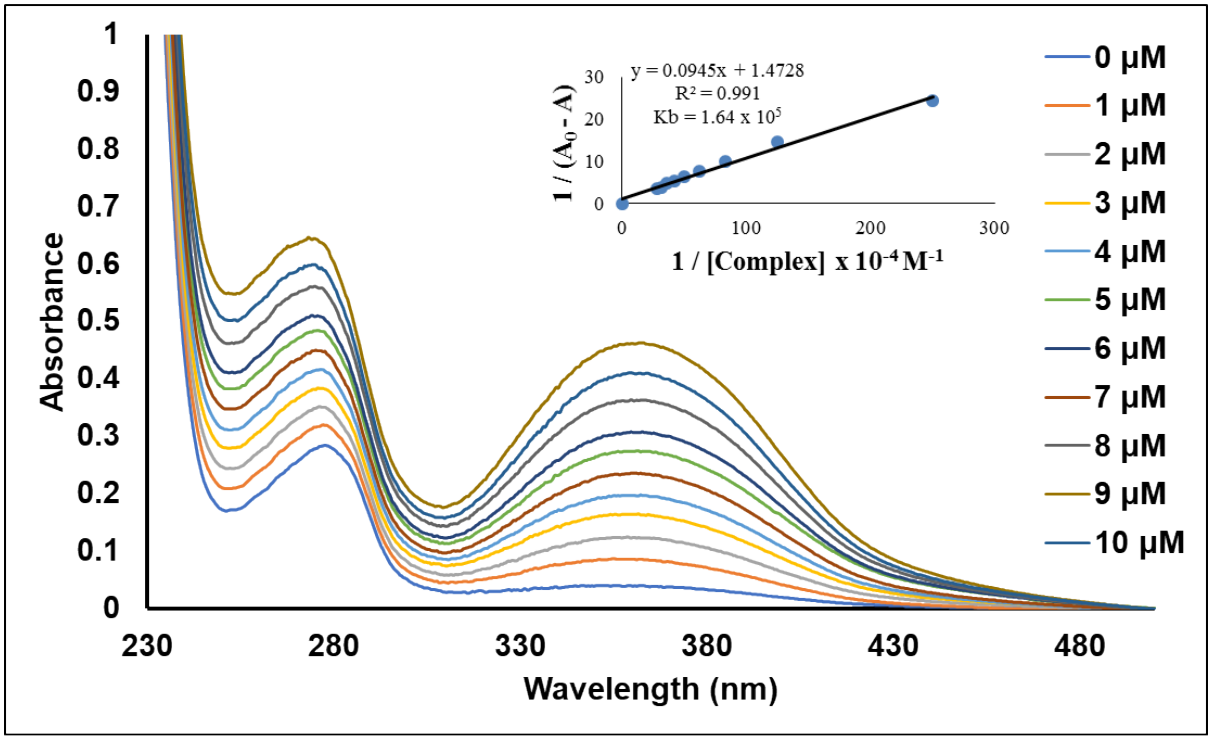

(b)

Figure S43: (a) Absorption spectra of **3h** in the absence and presence of increasing amounts of CT-DNA and (b) absorption spectra of BSA in the absence and presence of increasing amounts of **3h**.

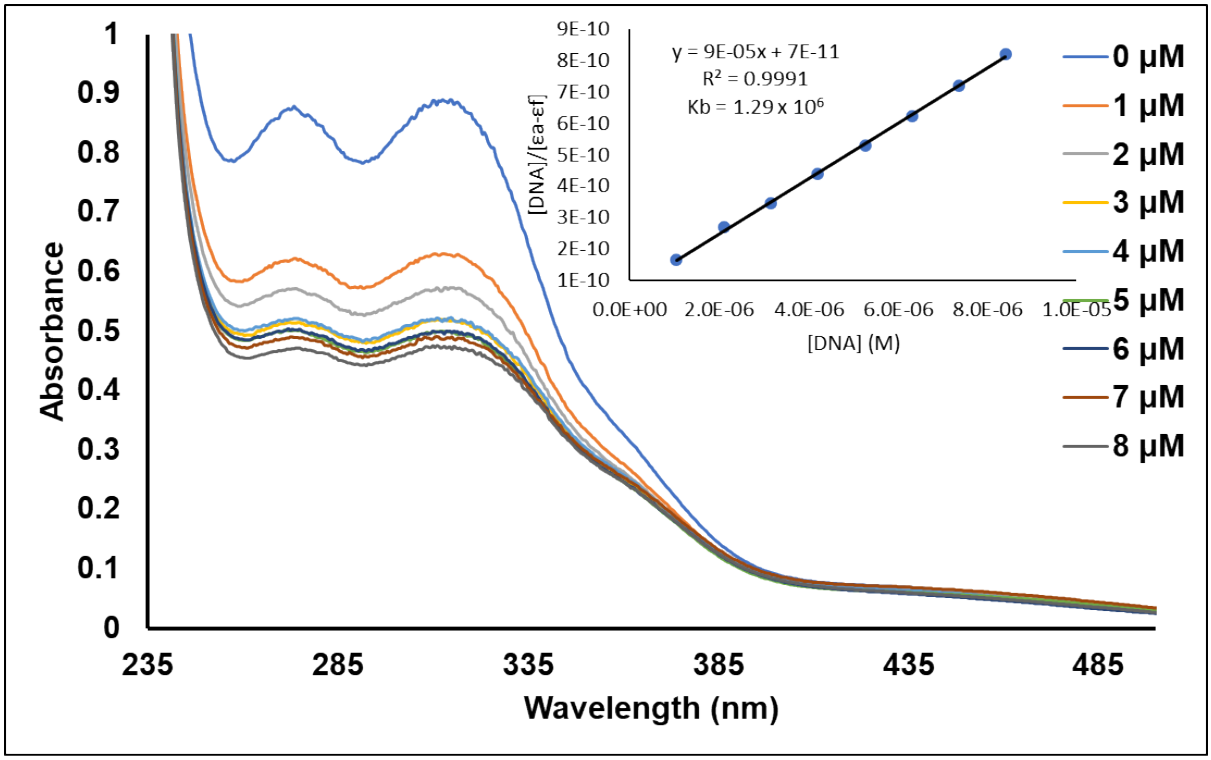

(a)

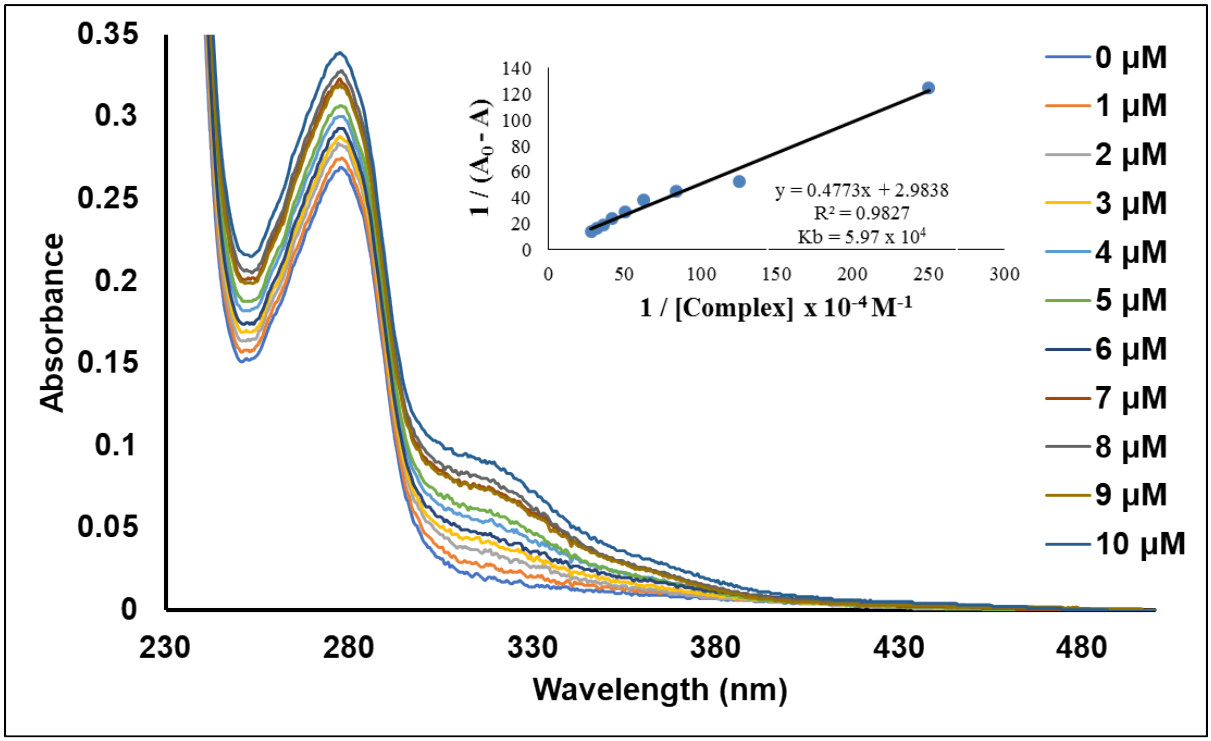

(b)

Figure S44: ((a) Absorption spectra of **3i** in the absence and presence of increasing amounts of CT-DNA and (b) absorption spectra of BSA in the absence and presence of increasing amounts of **3i**.

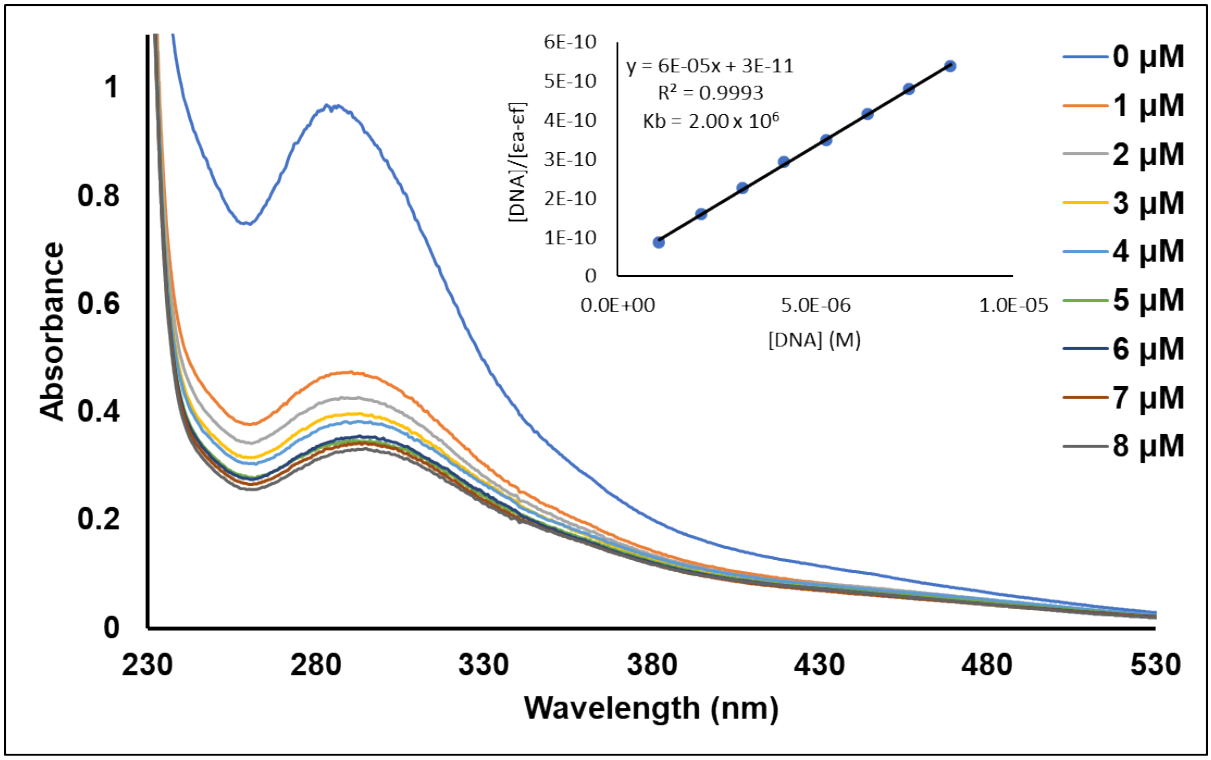

(a)

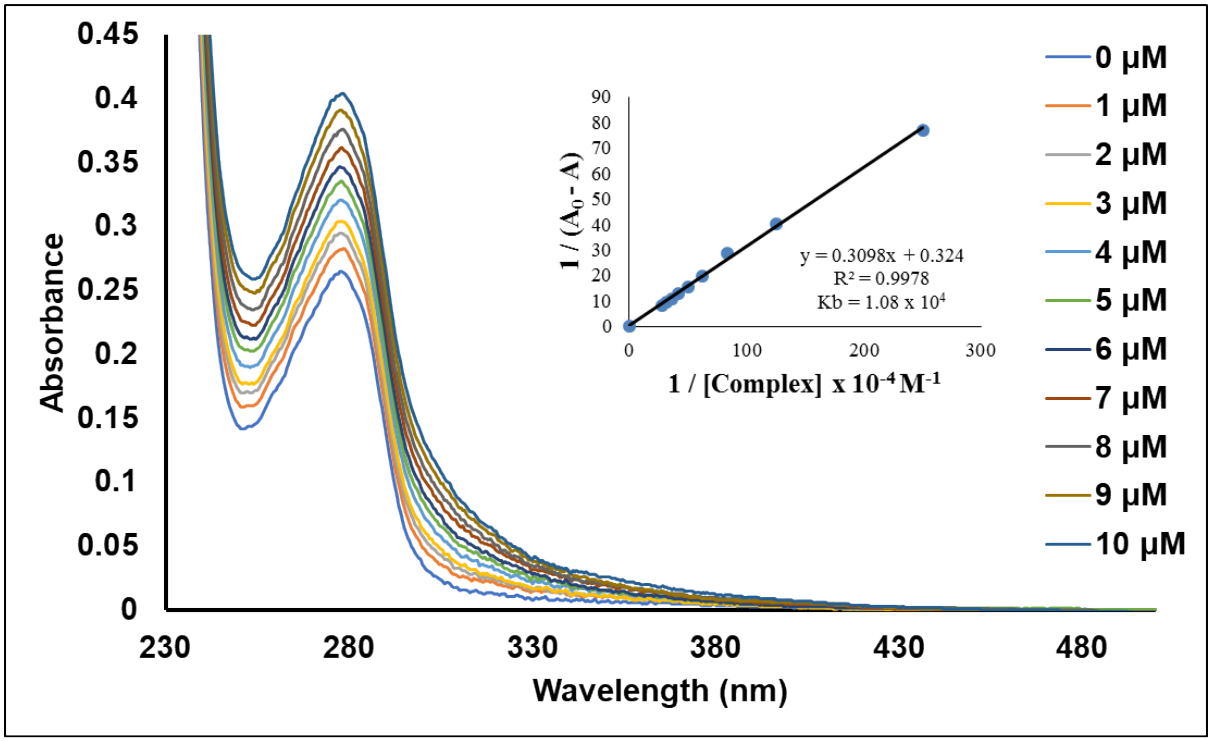

(b)

Figure S45: (a) Absorption spectra of **3j** in the absence and presence of increasing amounts of CT-DNA and (b) absorption spectra of BSA in the absence and presence of increasing amounts of **3j**.

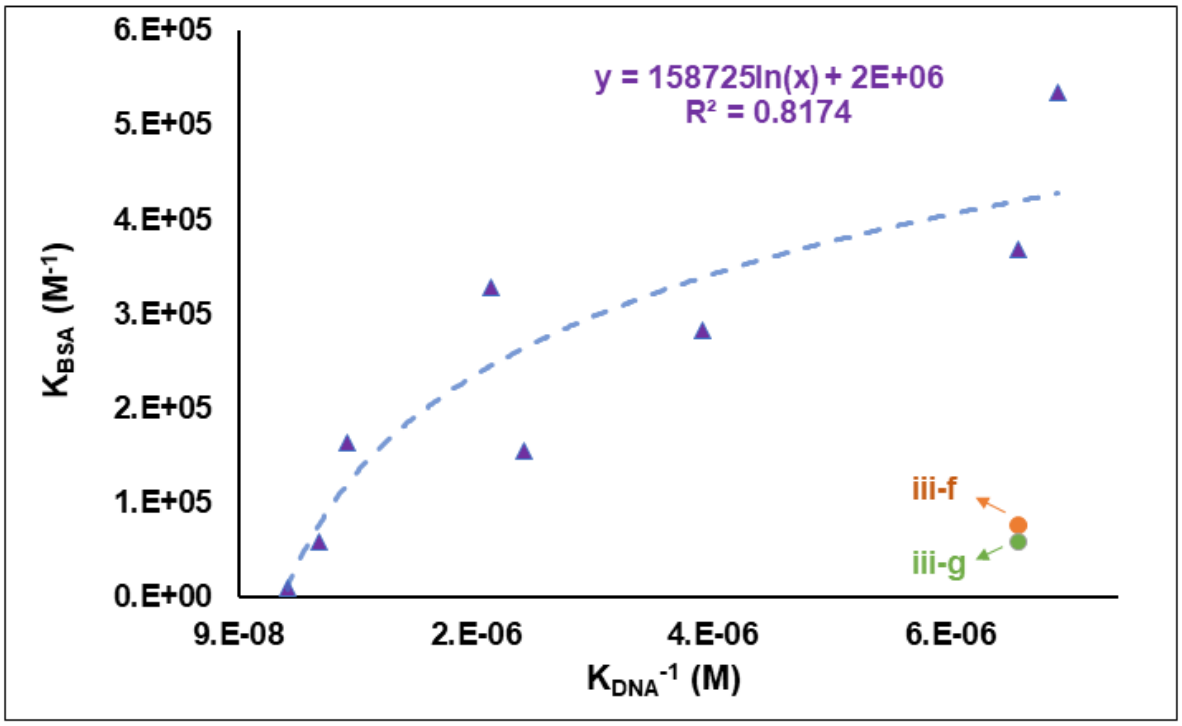

(a)

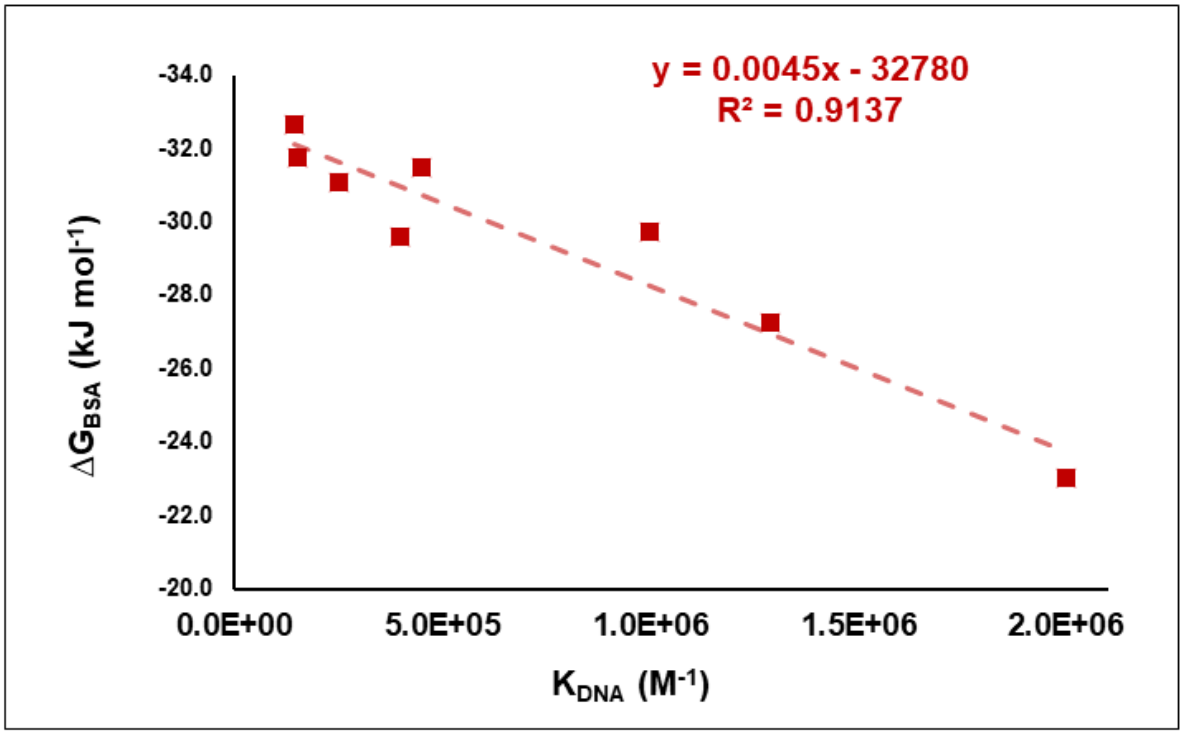

(b)

Figure S46: (a) K_{DNA}^{-1} versus K_{BSA} and (b) K_{DNA} versus ΔG_{BSA}. The associated data points, trendline and equation have the same colour coding. Compounds **3f** and **3g** are outliers and were omitted when generating the trendlines in (a) and (b).